Simulation and analysis of E325 ρ/ω spectra

E16 workshop @ Taiwan

240909

W. Nakai

Contents

Introduction

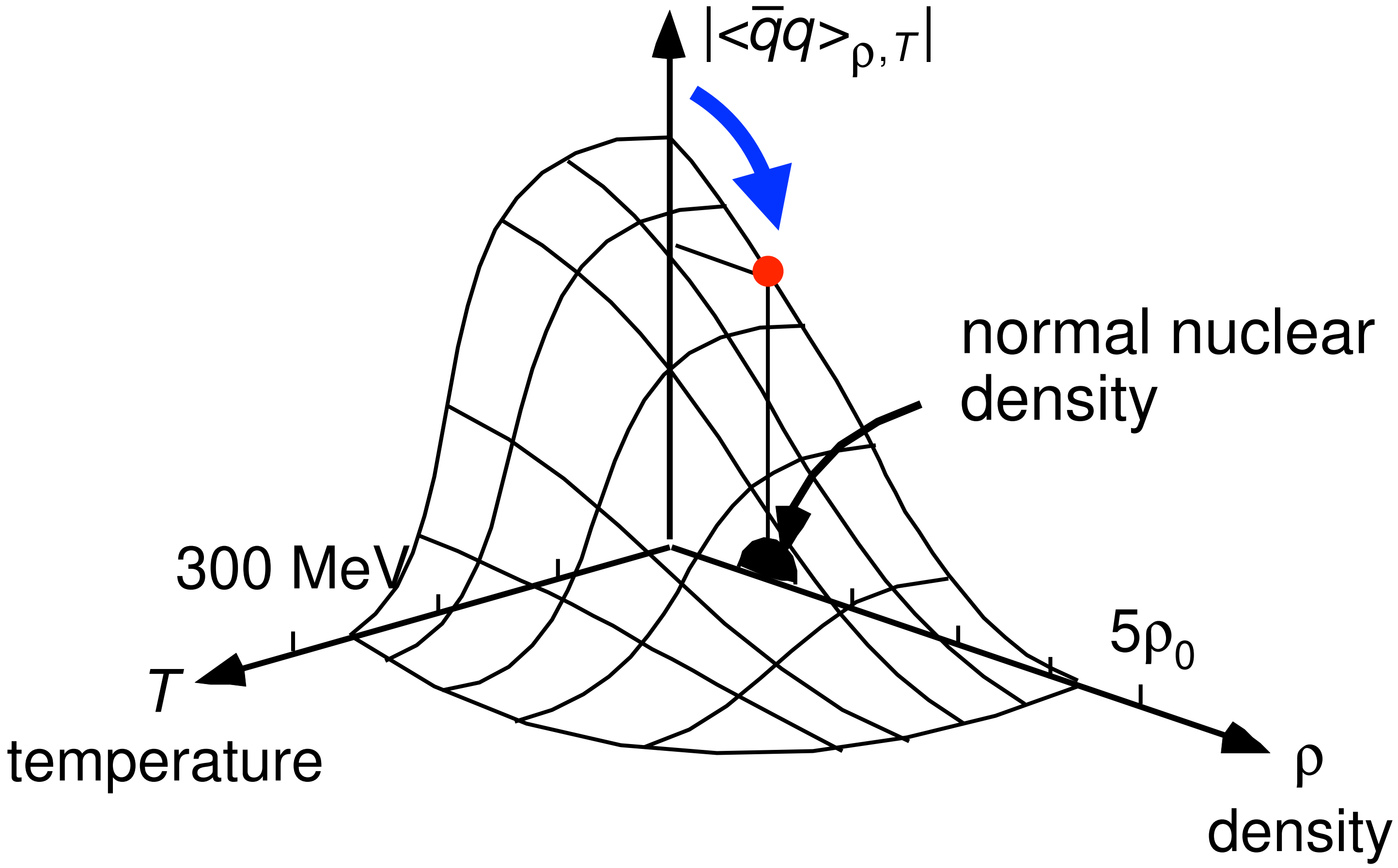

W. Weise, Nucl. Phys. A 553 (1993) 59-72.

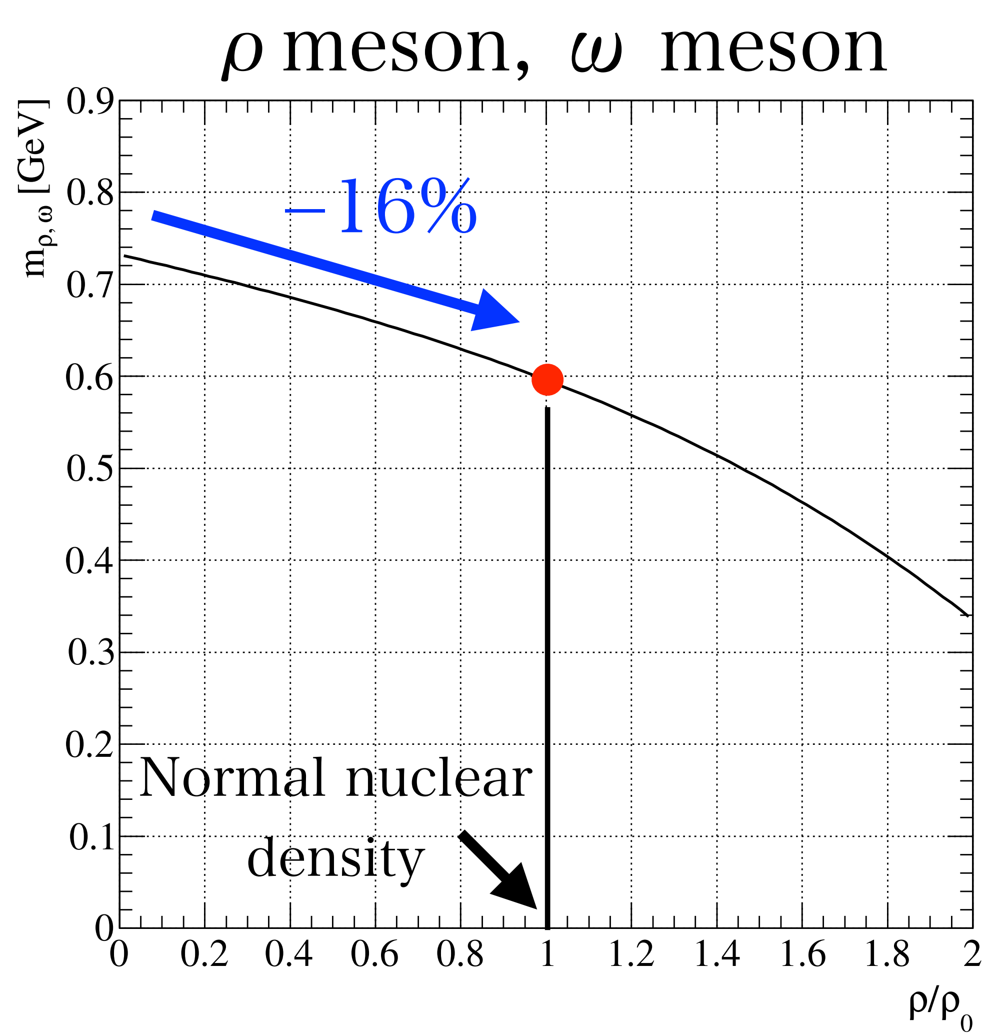

T. Hatsuda and S. H. Lee, Phys. Rev. C 46 (1992) R34.

- The origin of the hadron mass is the spontaneous breaking of chiral symmetry.
- Under finite density and/or temperature, the symmetry is partially restored.
- According to the QCD sum rule, the mass of the ρ/ω meson is **reduced by 16%** at the normal nuclear density.

Previous experiments (CLAS, 2008)

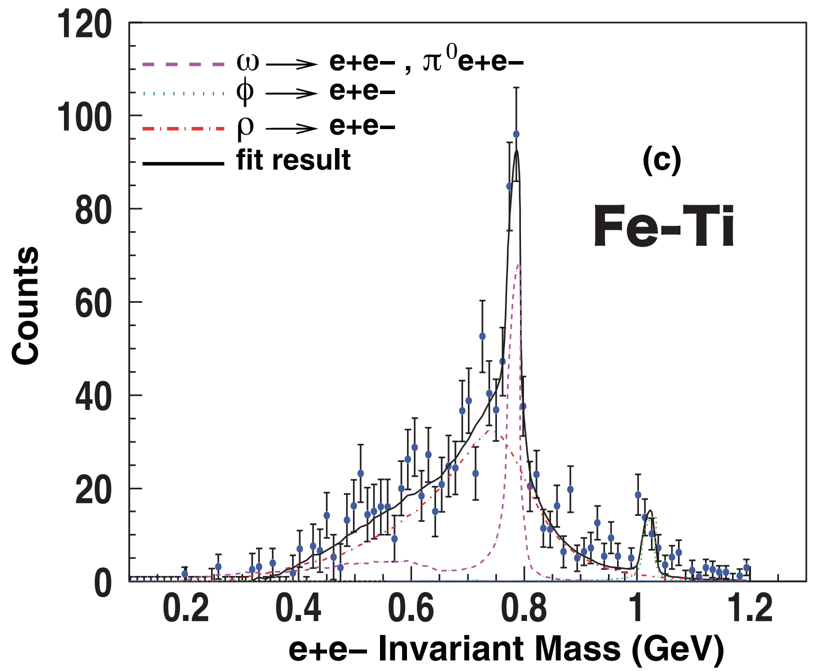

Subtract ω and ϕ components →

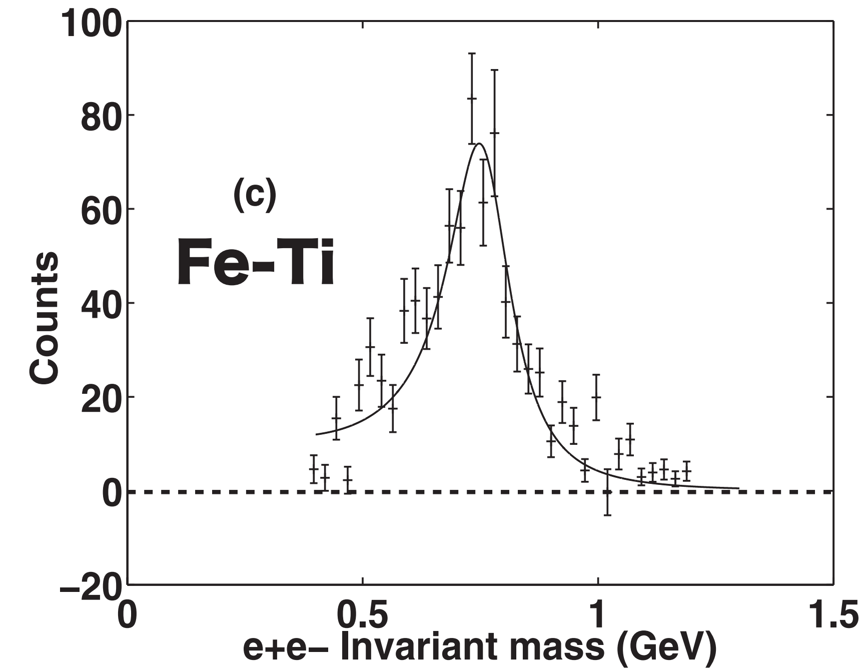

	Reaction	Channel	Method	Conclusion
CLAS [30]	γA	$\rho \to e^+e^-$	Mass shape	No mass shift, Broadening
CLAS [31]	γA	$\omega \to e^+e^-$	Transparency ratio	Broadening (> 200 MeV/c^2)
CB/TAPS[32, 33]	γA	$\omega \to \pi^0\gamma$	Mass shape	Low sensitivity
CB/TAPS[34, 35]	γA	$\omega \to \pi^0\gamma$	Transparency ratio	Broadening (60-200 MeV/c^2)
KEK E325[17]	pA	$\rho/\omega \to e^+e^-$	Mass shape	Mass shift ($\sim 9\%$), No broadening

CLAS, PRL 105, 112301 (2010)

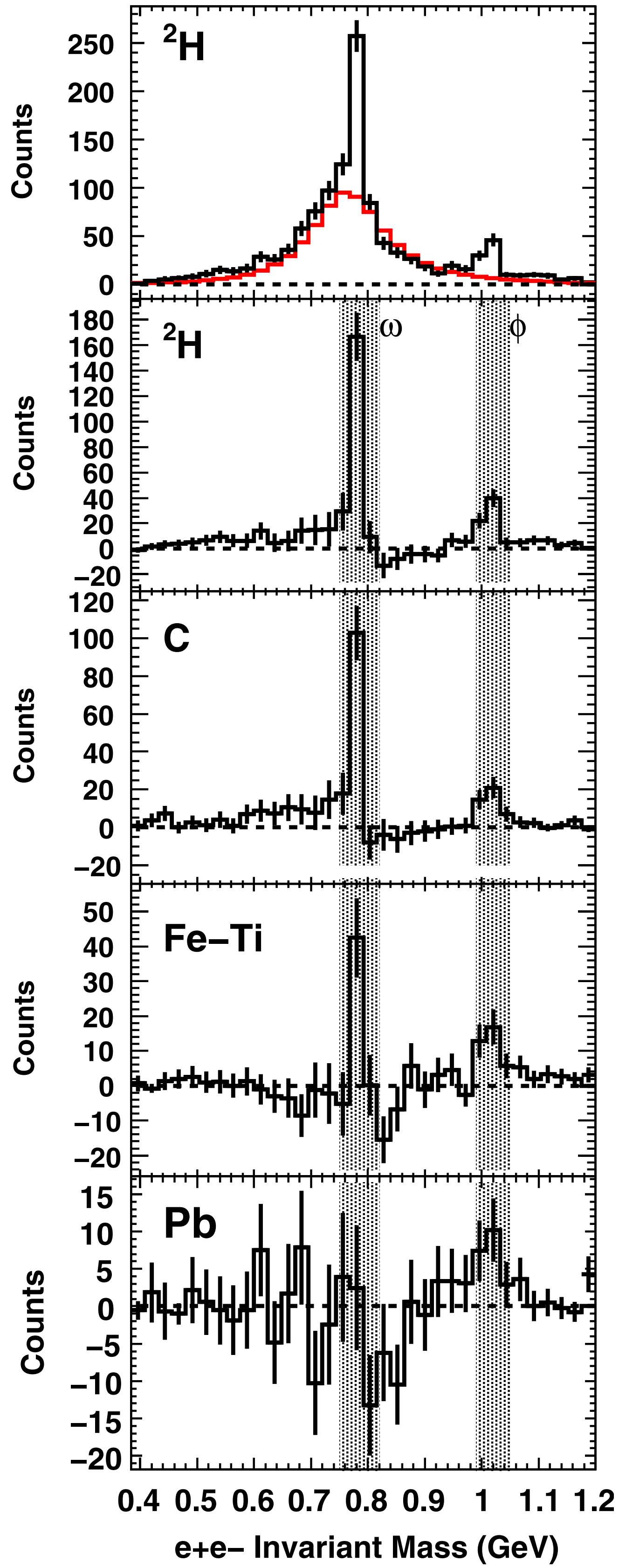

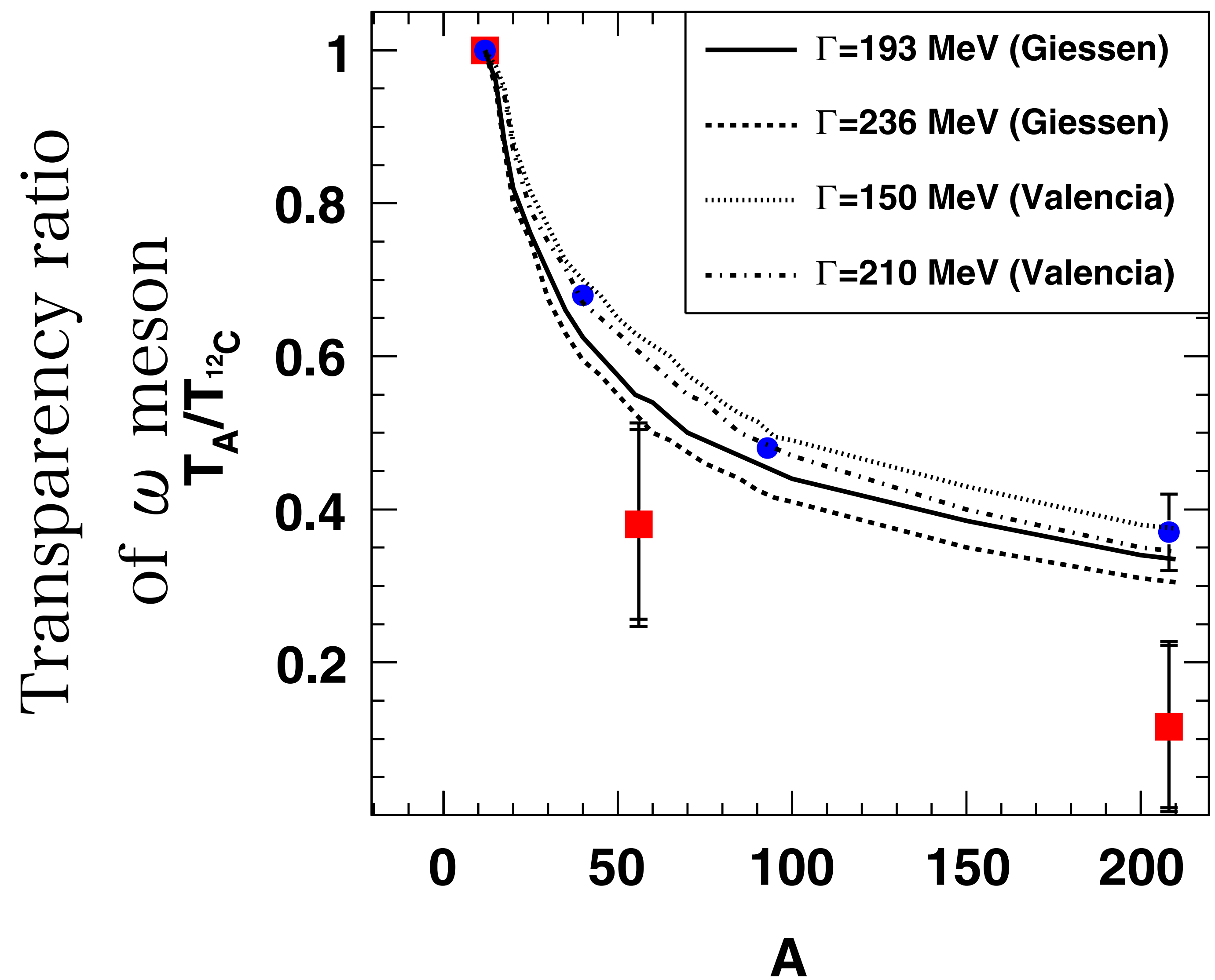

- Red: CLAS, Blue: TAPS
- The results indicate that the width broadening was greater than 200 MeV.

Previous experiments (TAPS, 2016)

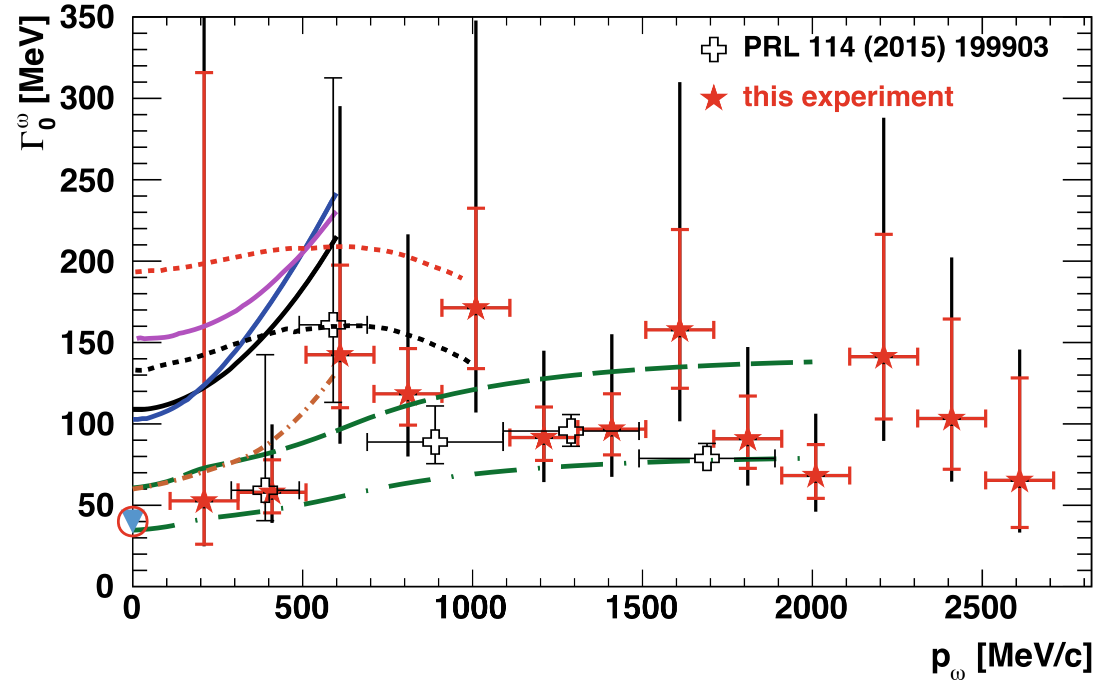

	Reaction	Channel	Method	Conclusion
CLAS [30]	γA	$\rho \to e^+e^-$	Mass shape	No mass shift, Broadening
CLAS [31]	γA	$\omega \to e^+e^-$	Transparency ratio	Broadening ($>$ 200 MeV/c^2)
CB/TAPS[32, 33]	γA	$\omega \to \pi^0\gamma$	Mass shape	Low sensitivity
CB/TAPS[34, 35]	γA	$\omega \to \pi^0\gamma$	Transparency ratio	Broadening (60-200 MeV/c^2)
KEK E325[17]	pA	$\rho/\omega \to e^+e^-$	Mass shape	Mass shift ($\sim$ 9%), No broadening

Previous results of the E325 (Naruki et al., 2006)

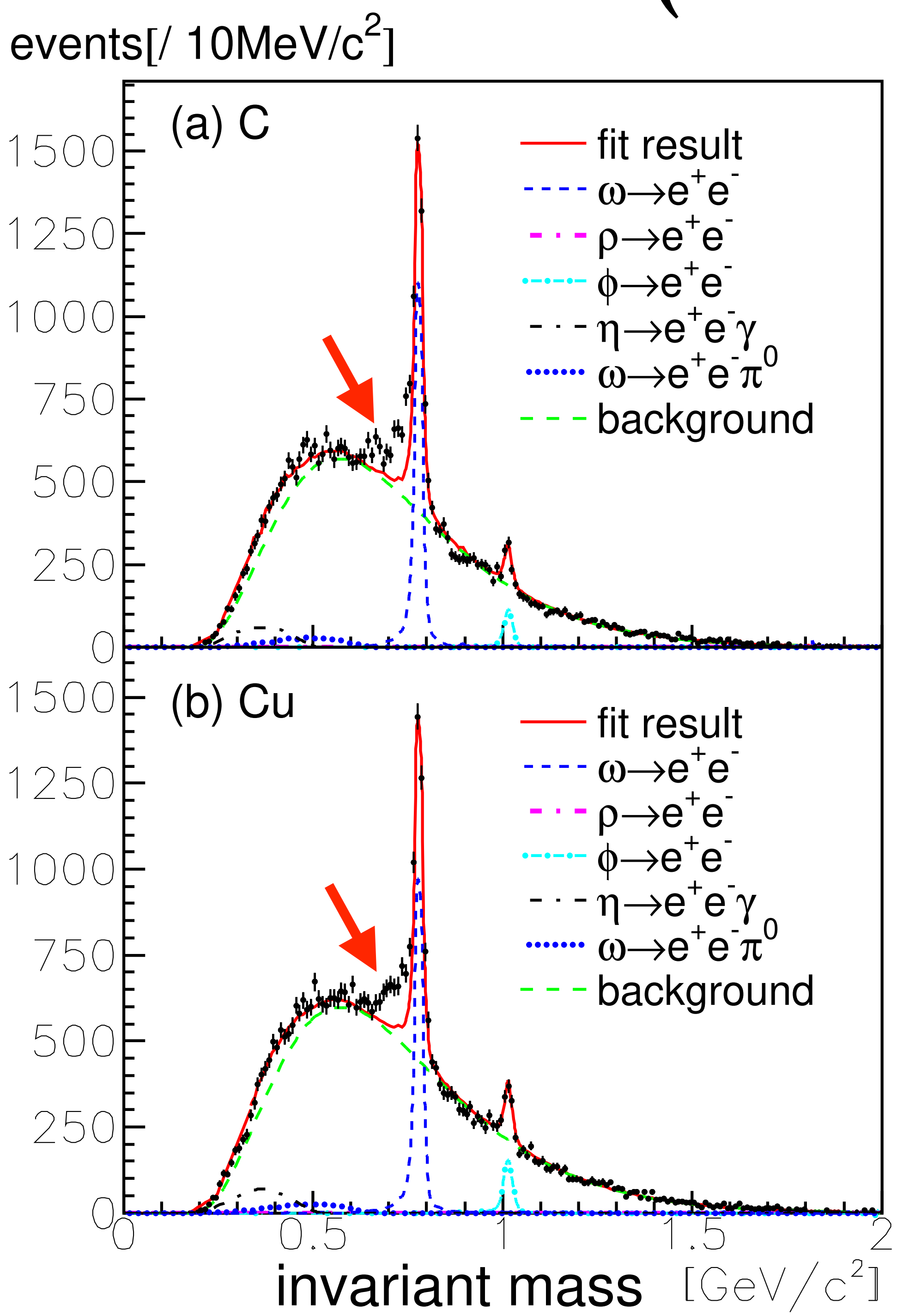

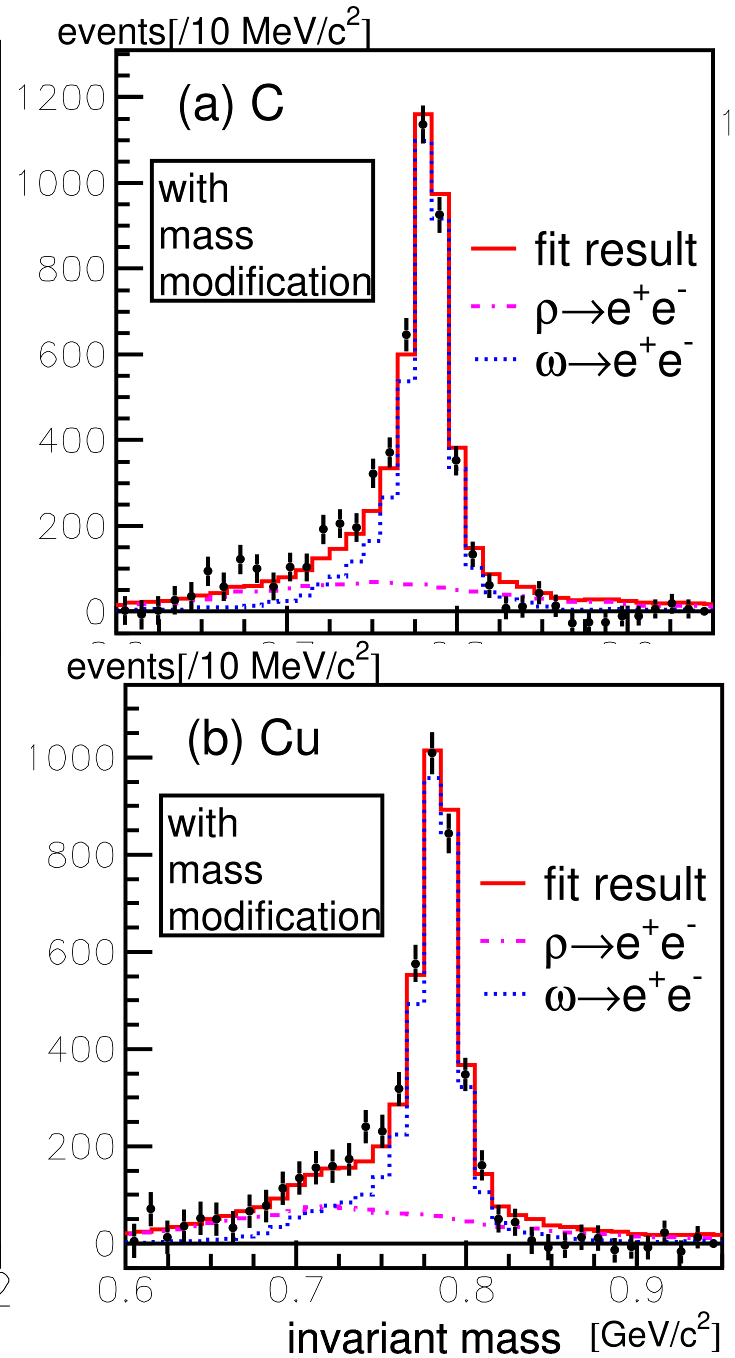

M. Naruki et al., Phys. Rev. Lett. 96 (2006) 092301.

- **Significant excesses were observed** at the left side of ω meson's peak.
- Model fit concludes
  - The masses of ρ/ω mesons are **reduced by about 9%**, and the widths are **not broadened**.

Present analysis

- To better understand these discrepancies, we conducted a re-analysis of the E325 data.
- To study $\beta\gamma$ -dependence, the improvement of statistics was needed.
  - Improved fiducial cut $\sim \times 2$
  - Increased dataset (Previous: 2002 data -> Present: 2001+2002 data) $\sim \times 1.5$
  - **The improvement was a factor of three.**
- The other updated points from the previous analysis
  - Internal radiative correction (IRC)
  - More recent form factors of Dalitz decay were used.
  - The asymmetric mass distribution function was applied in the model calculation.

Determination of the fiducial cut

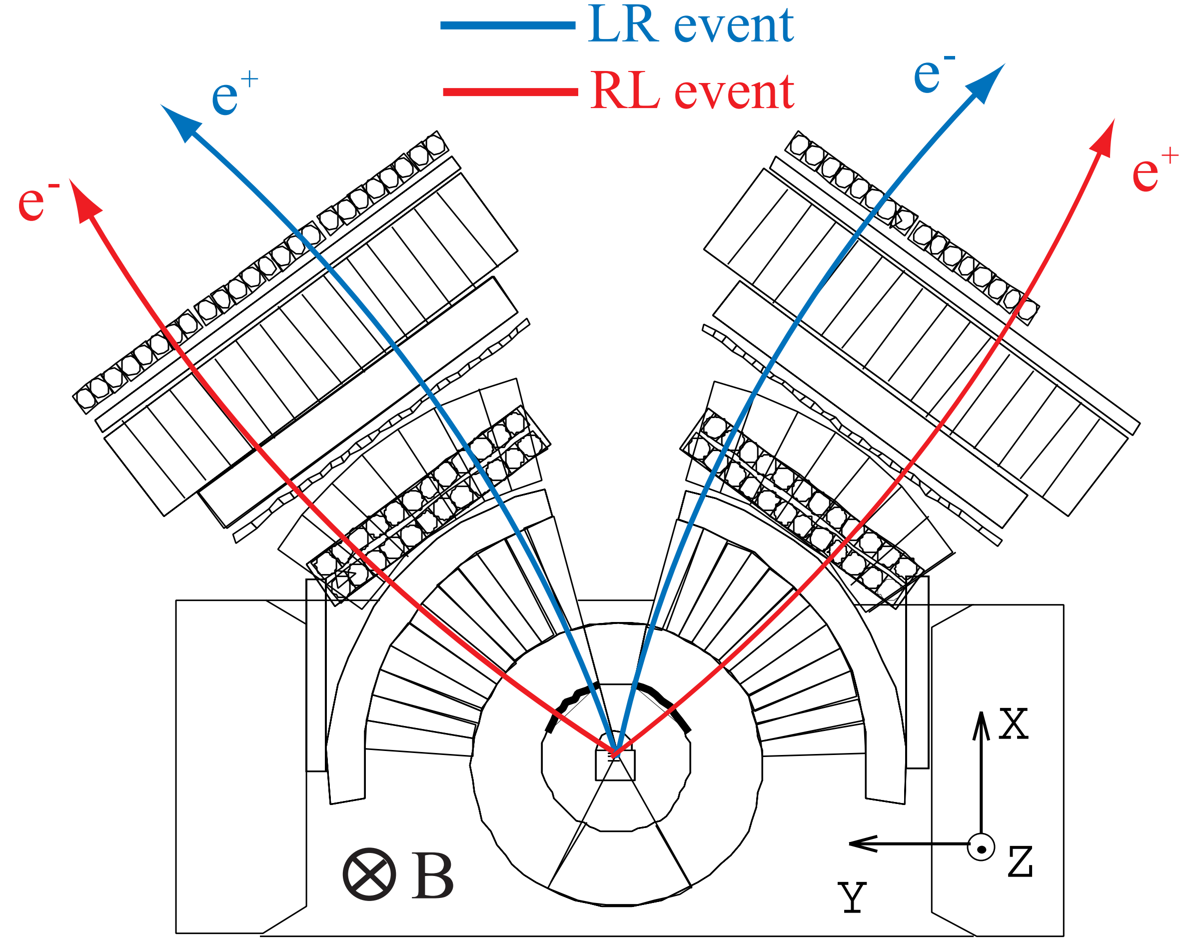

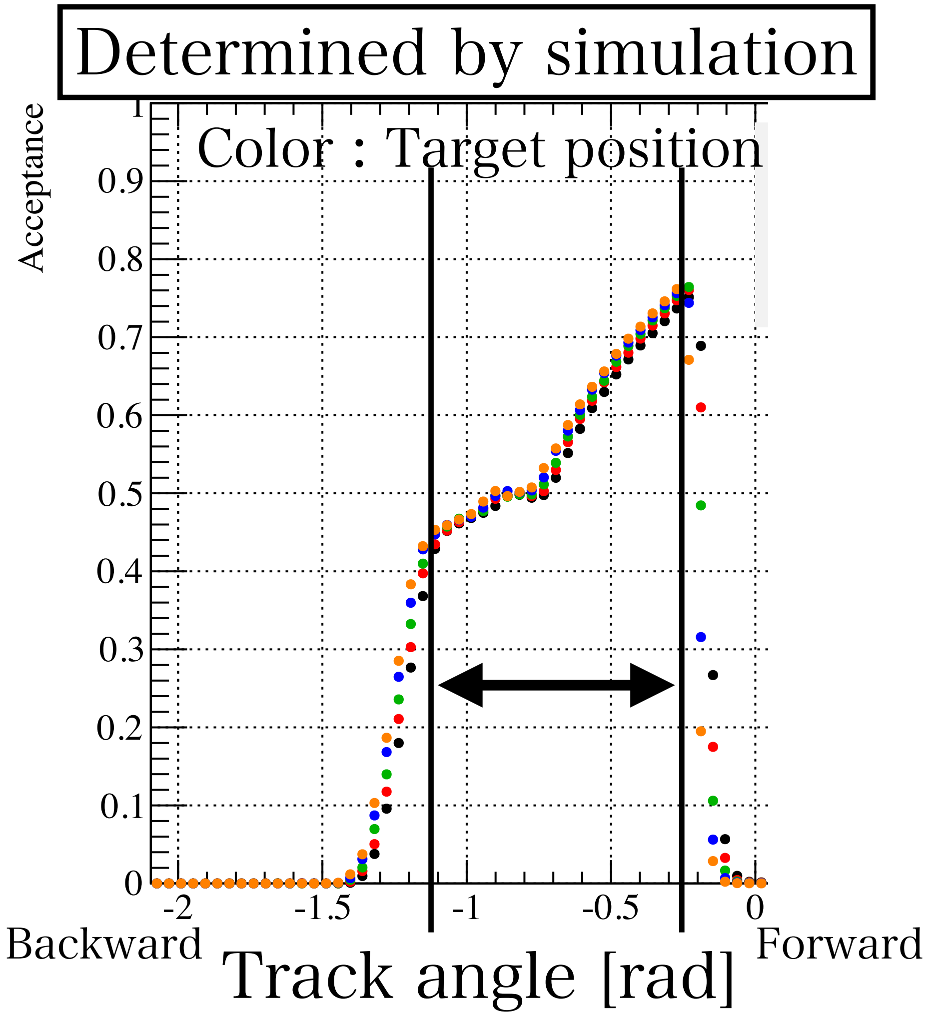

- The cut was applied by the angle of the track at the target position to align acceptances at all target locations.
- The cut values were determined based on simulation.

Determination of the fiducial cut

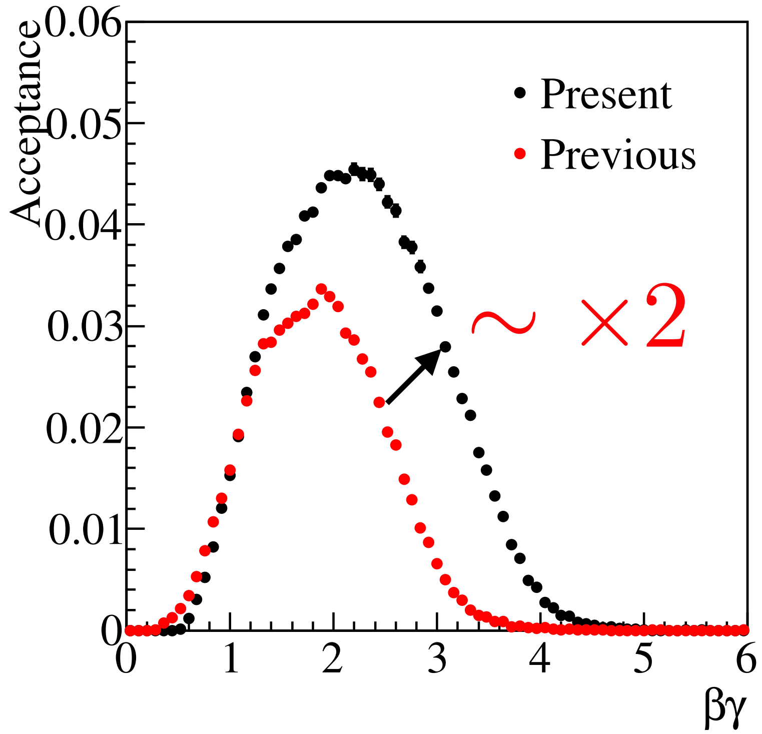

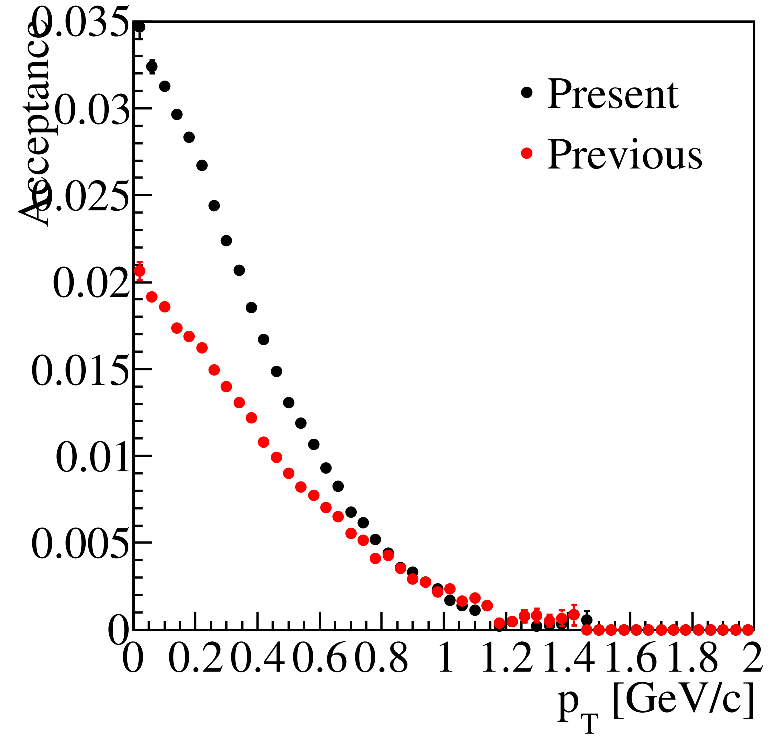

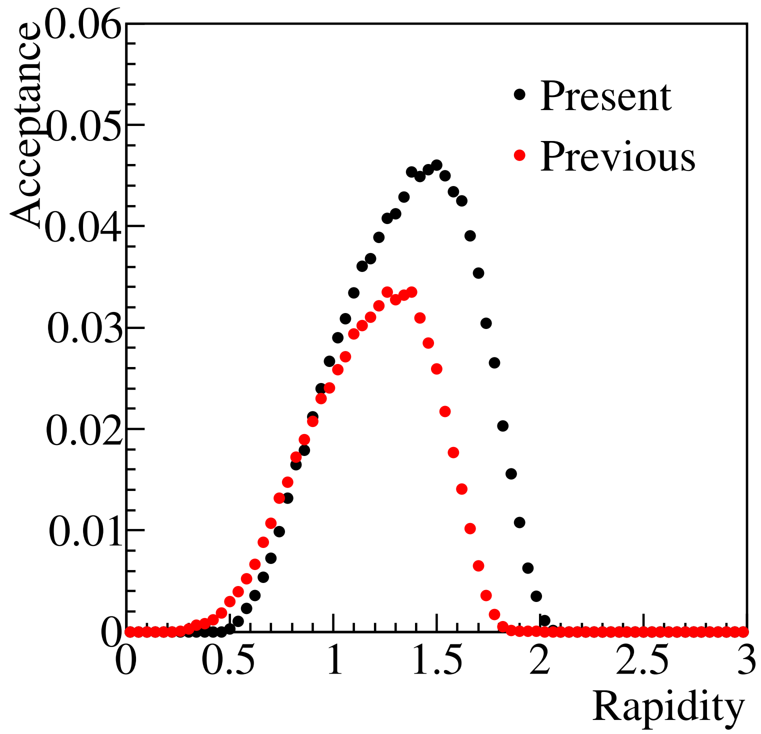

- We refined our analysis by optimizing kinematical cuts.
- The acceptance coverage of the detector was widened.
- As a result, the number of ω mesons was increased by a factor of 2.

Dalitz decay

I. Froehlich et al., PoS ACAT (2007) 076.

- Form factors of the Dalitz decays were calculated by “PLUTO”.
  - (Based on Vector Meson Dominance model)
- Helicity angle distribution $1+\cos^2\theta$ was used.

$\eta \rightarrow e^+e^-\gamma$

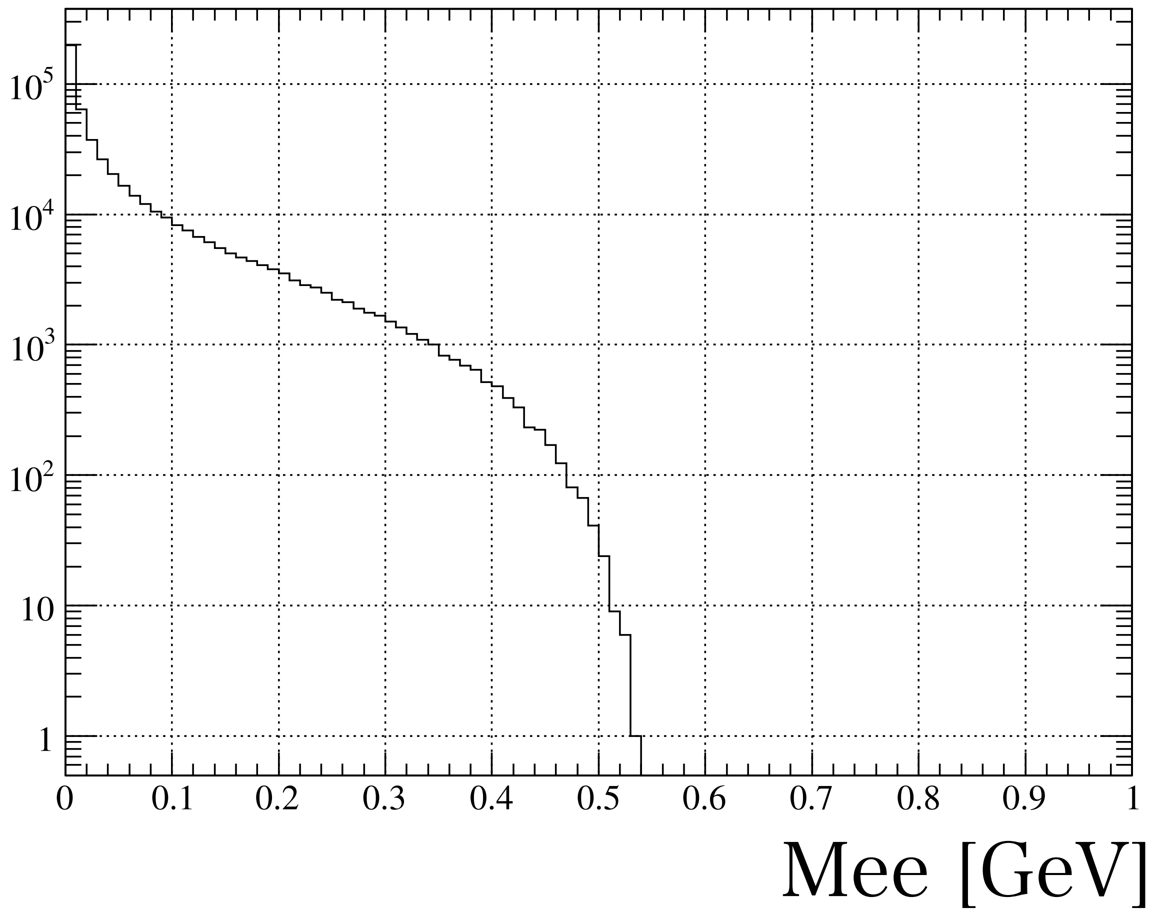

$\omega \rightarrow e^+e^-\pi^0$

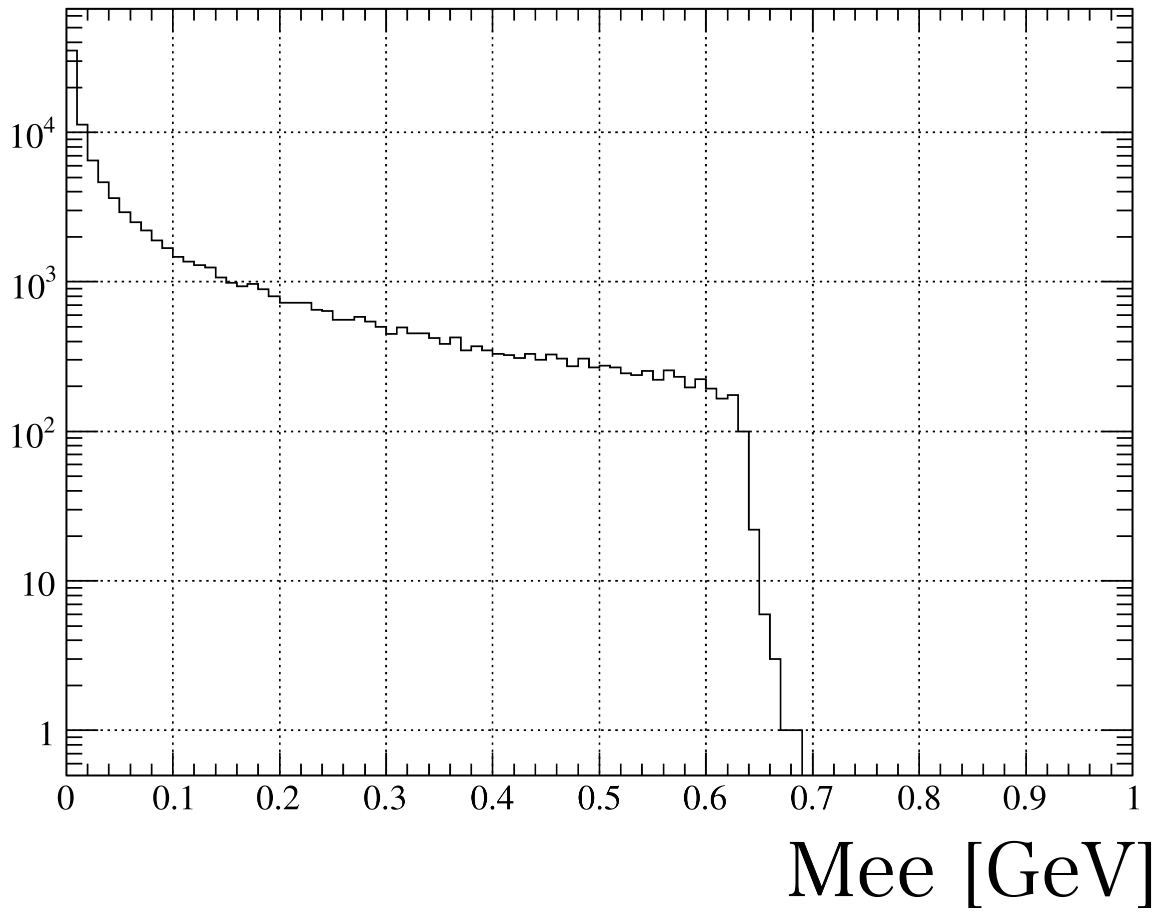

Internal radiative corrections (IRC)

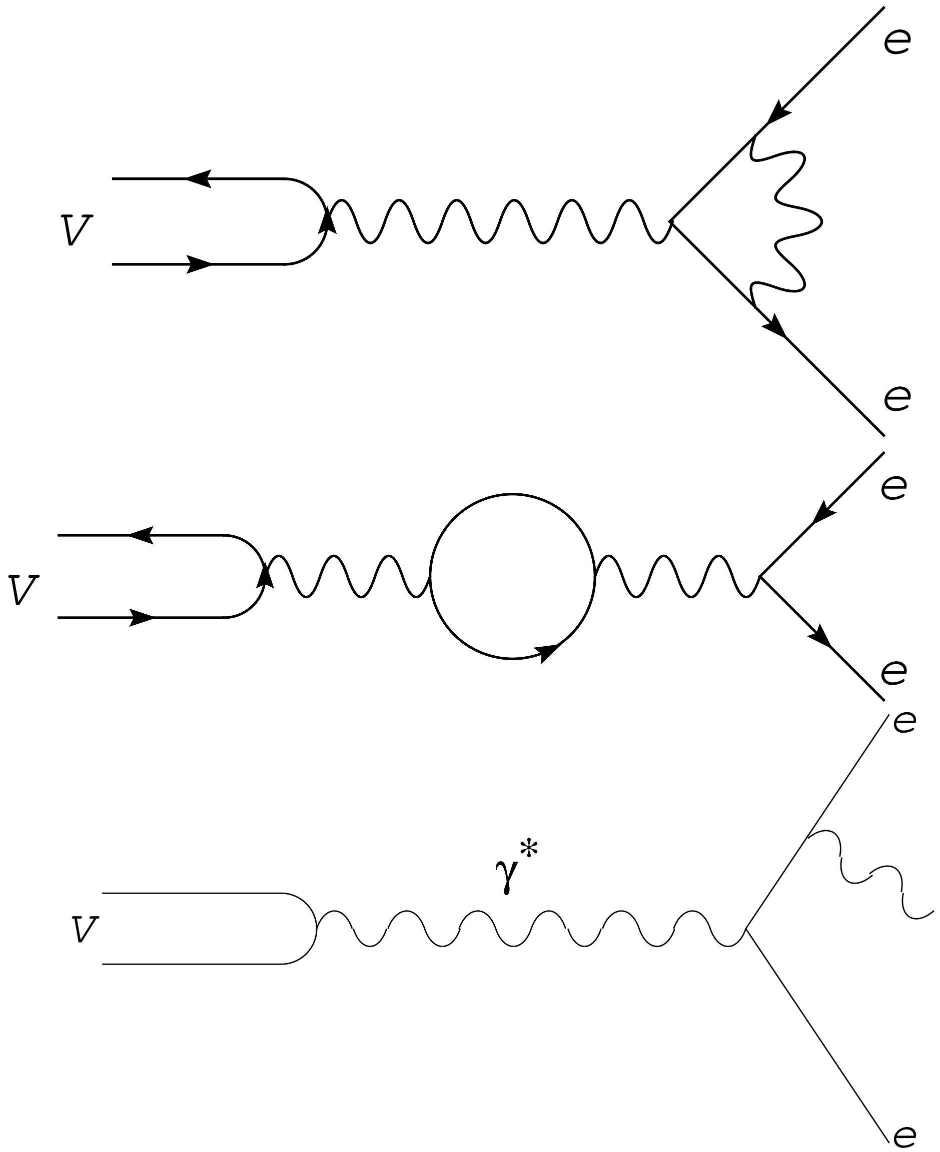

Final State Radiation

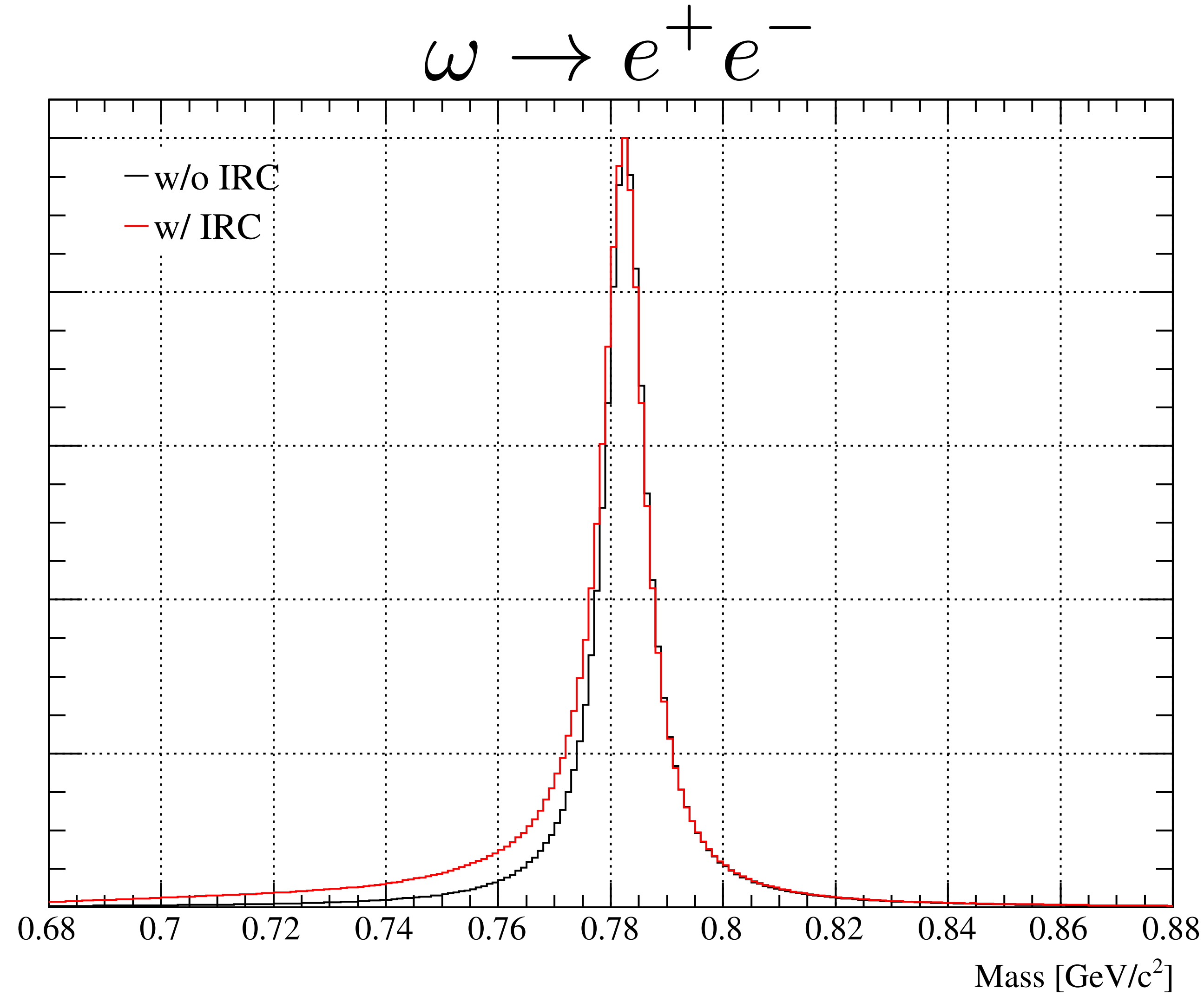

- The effect of QED correction was not applied in the previous analysis.
- Calculated by “PHOTOS” E. Barberio, B. van Eijk, and Z. Was, Comput. Phys. Commun. 66 (1991) 115.
- IRC was applied to not only two body decays but also Dalitz decays

Momentum and mass resolution of the E325 (Geant4)

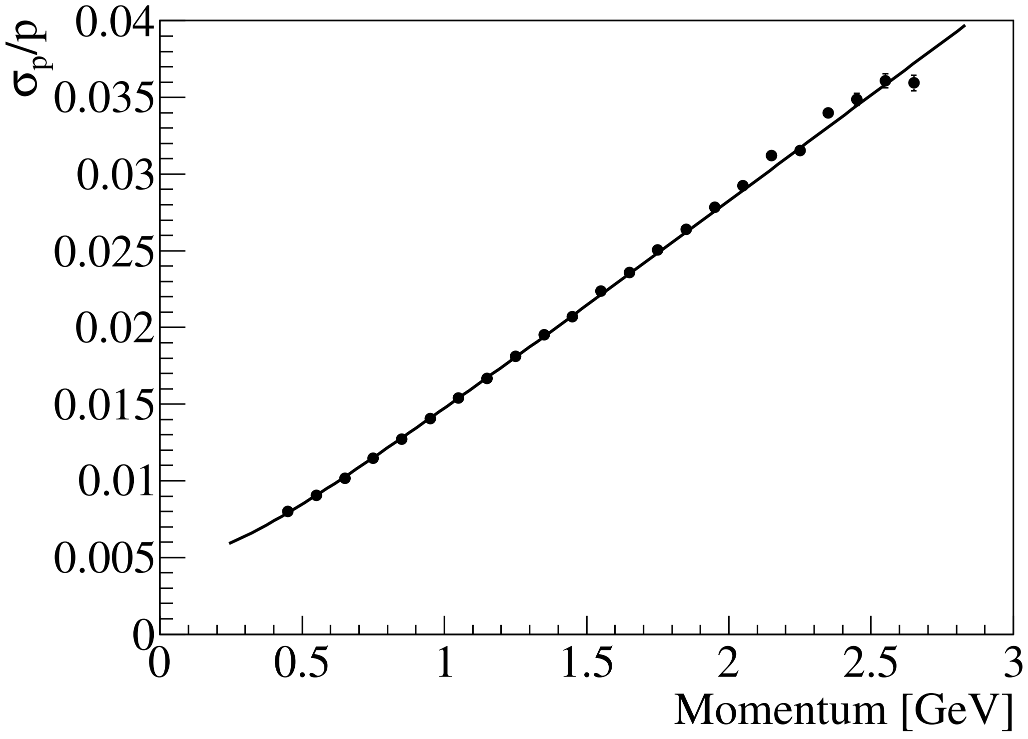

	ω
$\beta\gamma < 2.1$	6.4 ± 0.1 MeV/c^2
$2.1 < \beta\gamma < 2.7$	8.0 ± 0.1 MeV/c^2
$2.7 < \beta\gamma$	9.9 ± 0.1 MeV/c^2
all $\beta\gamma$	8.2 ± 0.1 MeV/c^2

- Tuned for the ω meson's peak (position and width)
- Momentum resolution

$$\sigma_p/p = \sqrt{(1.39\% \cdot p\ [\mathrm{GeV}/c])^2 + (0.49\%)^2}$$

- Mass resolution
  - about 8 MeV at omega meson's mass
- Well reproduced the obtained peak except for excess region

Mass spectra, Fit results

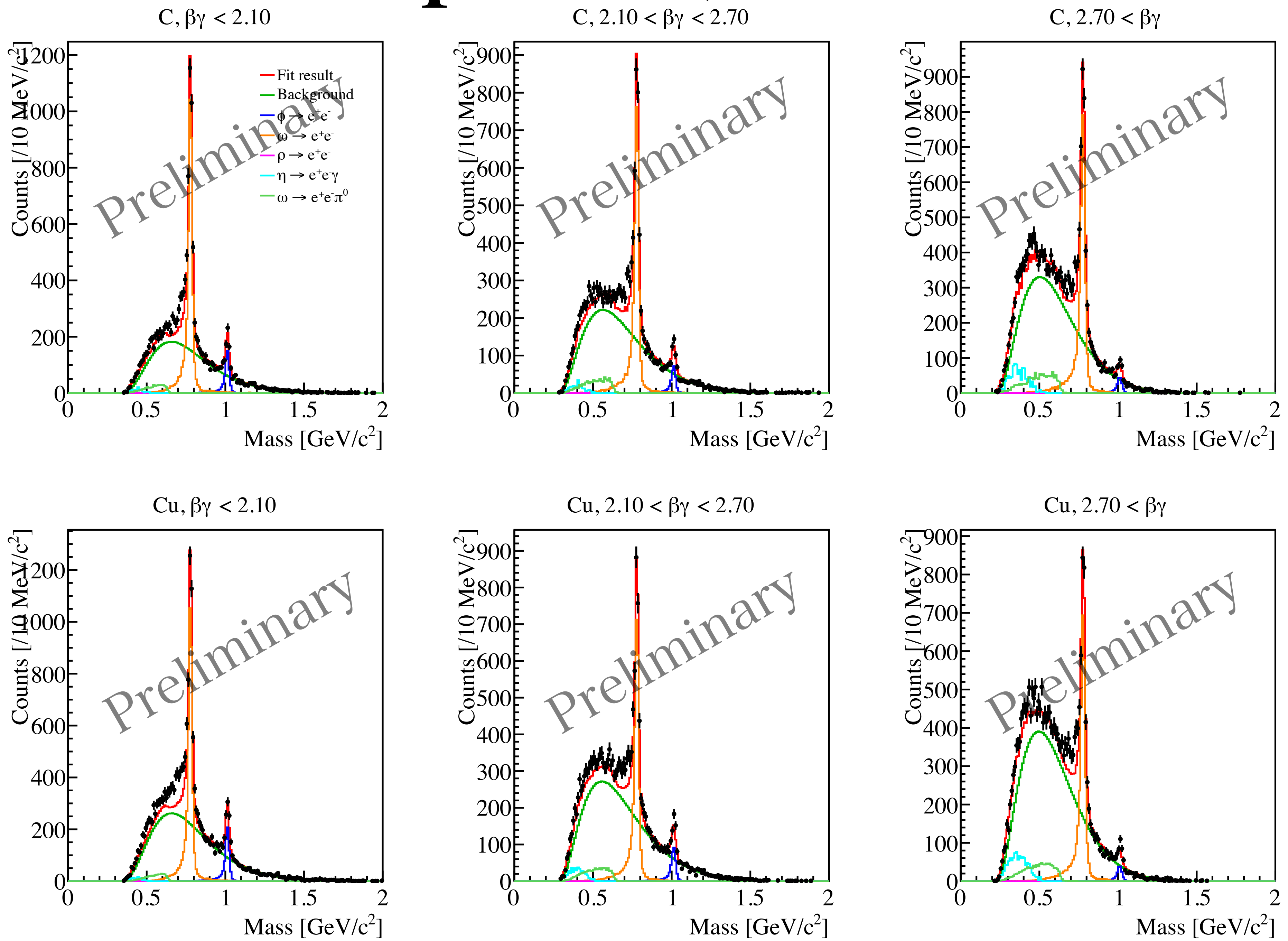

- The fitting results reproduce the data well except for the excess region.
- In this fit, the amplitude of ρ meson (Magenta) is consistent with 0.
- χ^2 values are summarized on the next page.

Fit results

Table 12 χ^2/ndf and its probability values from the fitting process, (a) including and (b) excluding the excess region.

(a) Include, $p < 0.01$ (b) Exclude, $p > 0.01$

		χ^2/ndf (a)	Probability (a)	χ^2/ndf (b)	Probability (b)
C	$\beta\gamma < 2.1$	334.3/221	1.3e-06	186.8/193	0.61
	$2.1 < \beta\gamma < 2.7$	322/206	4.1e-07	184.9/178	0.35
	$2.7 < \beta\gamma$	247.2/160	1.2e-05	132.9/132	0.46
Cu	$\beta\gamma < 2.1$	892.9/628	1.5e-11	613.6/544	0.020
	$2.1 < \beta\gamma < 2.7$	707.7/537	9.6e-07	519.9/453	0.016
	$2.7 < \beta\gamma$	507.8/418	0.0017	333.7/334	0.49

Table 13 Yield of ω mesons, the number of excess instances, significance of excess, and excess ratio.

$> 8\,\sigma$ for all regions

		N_ω	N_{excess}	significance	excess ratio $\frac{N_{\text{excess}}}{N_\omega + N_{\text{excess}}}$
C	$\beta\gamma < 2.1$	4278 ± 98	836 ± 98	8.5σ	0.16 ± 0.019
	$2.1 < \beta\gamma < 2.7$	3394 ± 84	802 ± 82	9.8σ	0.19 ± 0.019
	$2.7 < \beta\gamma$	3848 ± 106	771 ± 90	8.6σ	0.17 ± 0.020
Cu	$\beta\gamma < 2.1$	4271 ± 96	1310 ± 98	13.4σ	0.23 ± 0.017
	$2.1 < \beta\gamma < 2.7$	3127 ± 82	890 ± 84	10.6σ	0.22 ± 0.021
	$2.7 < \beta\gamma$	3348 ± 90	909 ± 97	9.4σ	0.21 ± 0.022

Excess ratio vs $\beta\gamma$

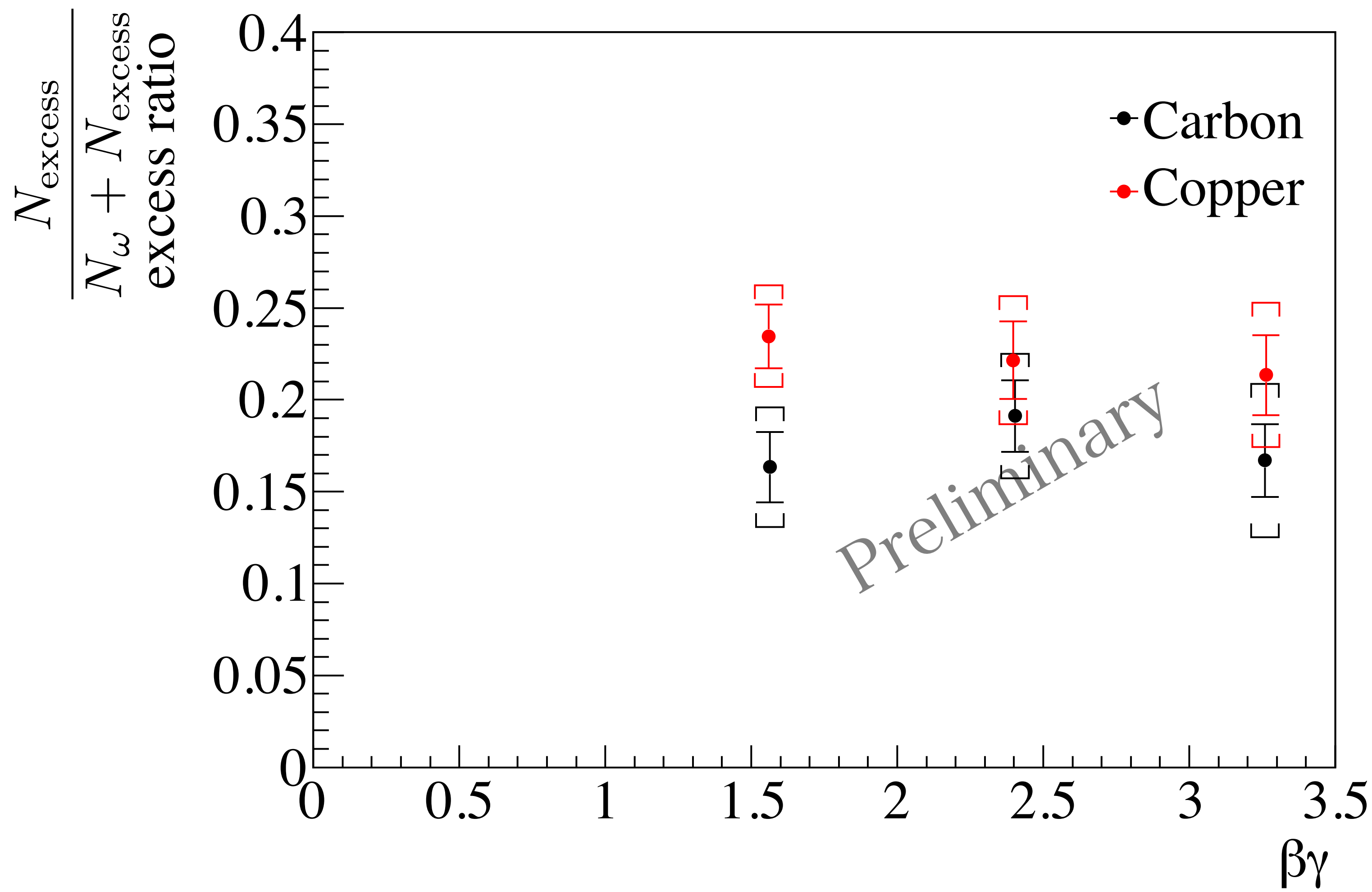

- I: Statistical error, [ ]: Systematic error
- Conclusions
  - **Significant excesses were observed for all targets and all $\beta\gamma$ regions.**
  - Clear $\beta\gamma$ -dependence was not observed.
- The excess ratios are affected by experimental effects.
  - **To interpret the excesses, some model calculation is needed.**

Model calculation (Generation point and Decay point)

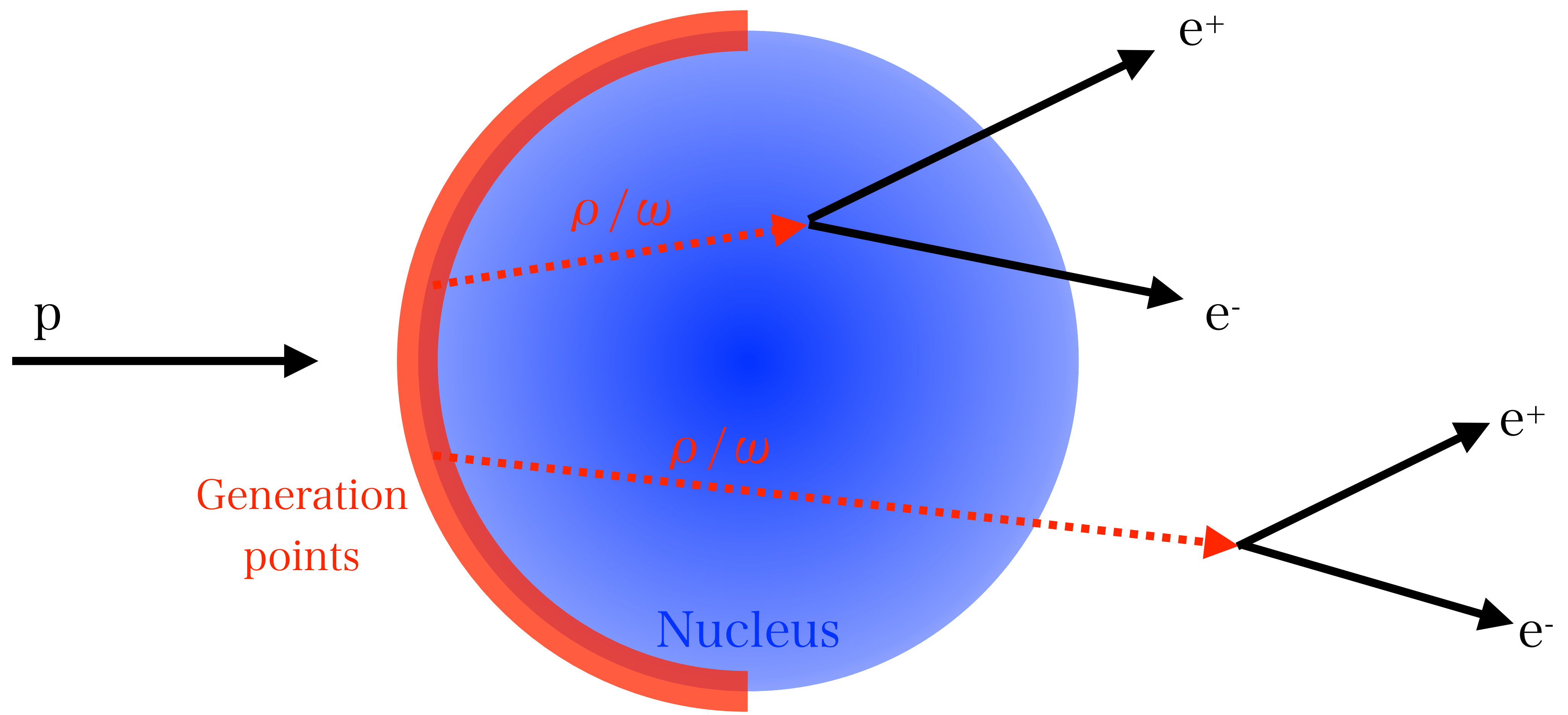

- $\sigma \propto A^{2/3}$

T. Tabaru et al., Phys. Rev. C 74, 025201 (2006).

- The production position distribution is on the nucleus's surface on the proton's incident side.
- Vector mesons were traced in 0.1 fm steps and decayed with a width and mass that depends on the density.
- $$m(\rho) = \left(1 - k_1 \frac{\rho}{\rho_0}\right) m(0) \qquad \Gamma(\rho) = \left(1 + k_2 \frac{\rho}{\rho_0}\right) \Gamma(0)$$

Mass shape formulae

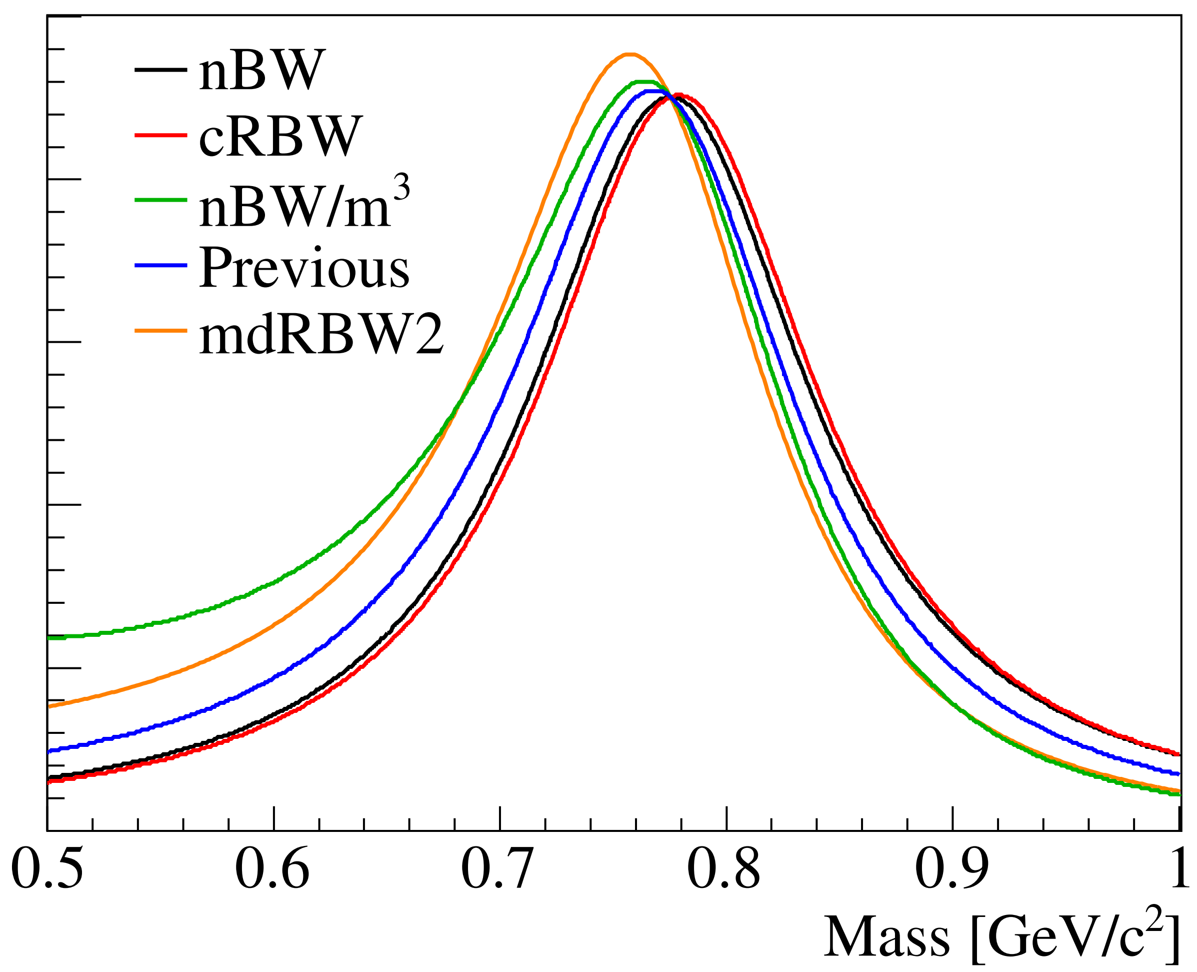

- Non-relativistic Breit-Wigner (nBW)
- constant width and mass-dependent width relativistic Breit-Wigner
- CLAS used nBW/m^3 as an approximation of mass-dependent Breit-Wigner.
- **We tested two extreme cases: nBW (case (i)) and nBW/m^3 (case (ii)).**

Case (i): nBW

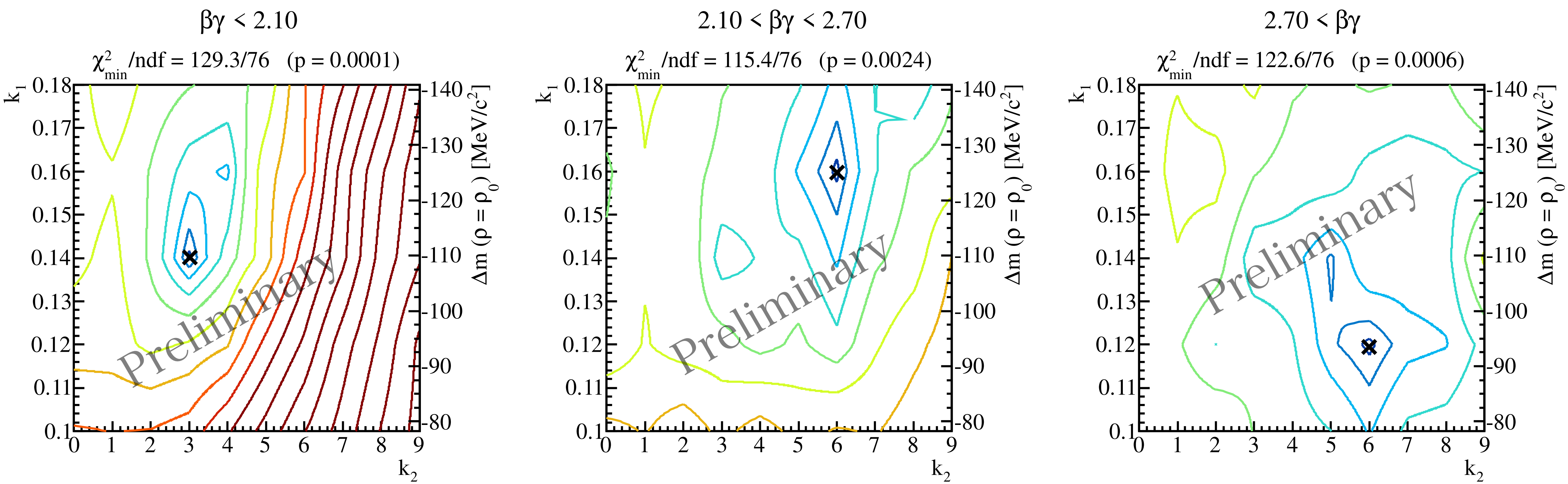

- Model fitting was performed with grid points in 0.02 steps for k1 and 1.0 for k2.
- The contours correspond to $\Delta\chi^2 = 1, 4, 9, \cdots$
- The k1 and k2 parameters were common for C, Cu, ω, ρ.
- In case (i), the minimum around k2 = 3 - 6.

Case (i): nBW

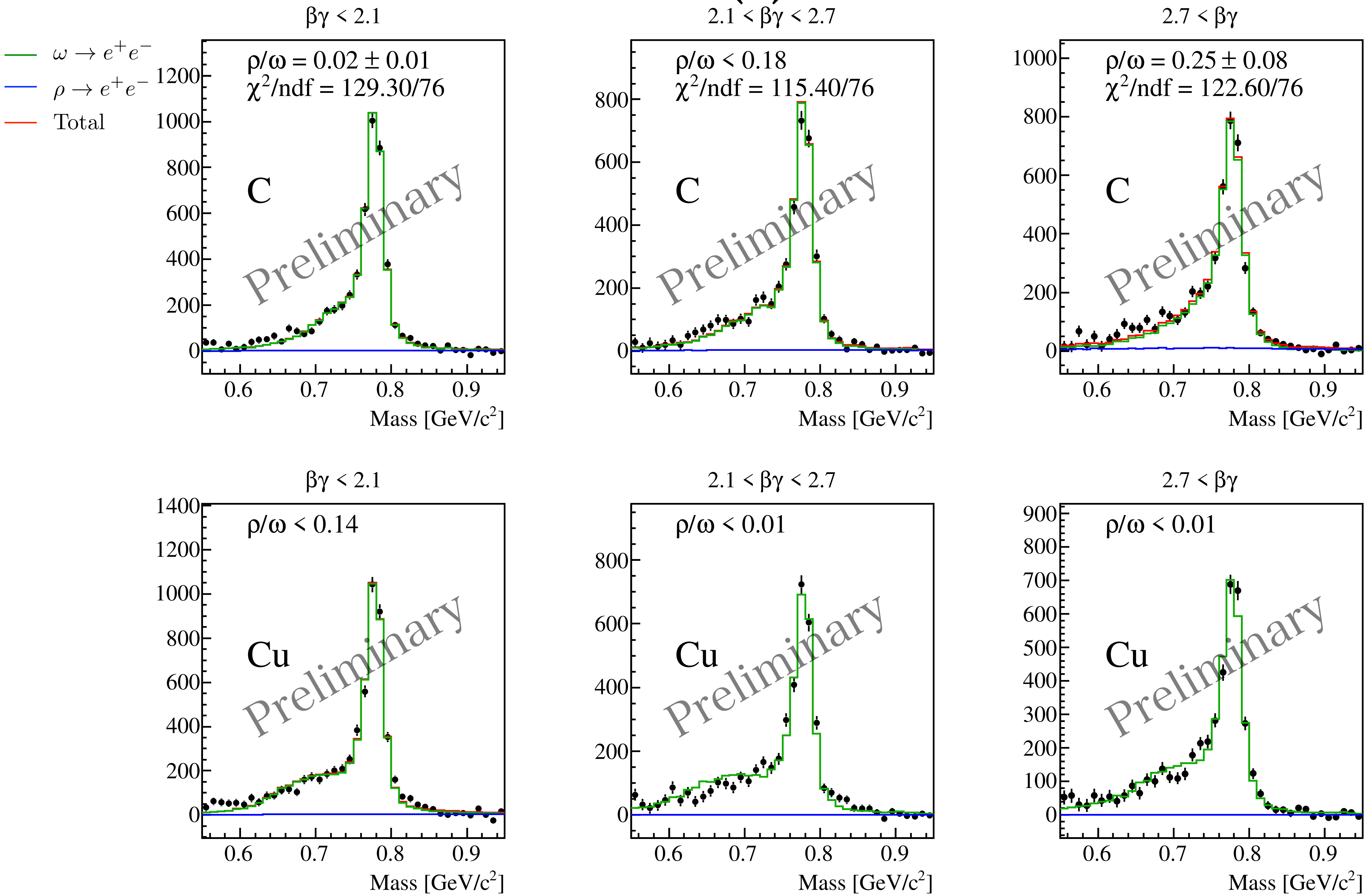

- Fit results at k1 and k2 that minimize $\chi 2$.
- The result of ρ/ω ~ 0 contradicts a previous 12 GeV p+p measurement.
  - $\sigma_{\omega}/\sigma_{\rho}$ = 1.0 +- 0.2 (V. Blobel et al., Phys. Lett. B48, 73 (1974))

Case (ii): nBW/m³

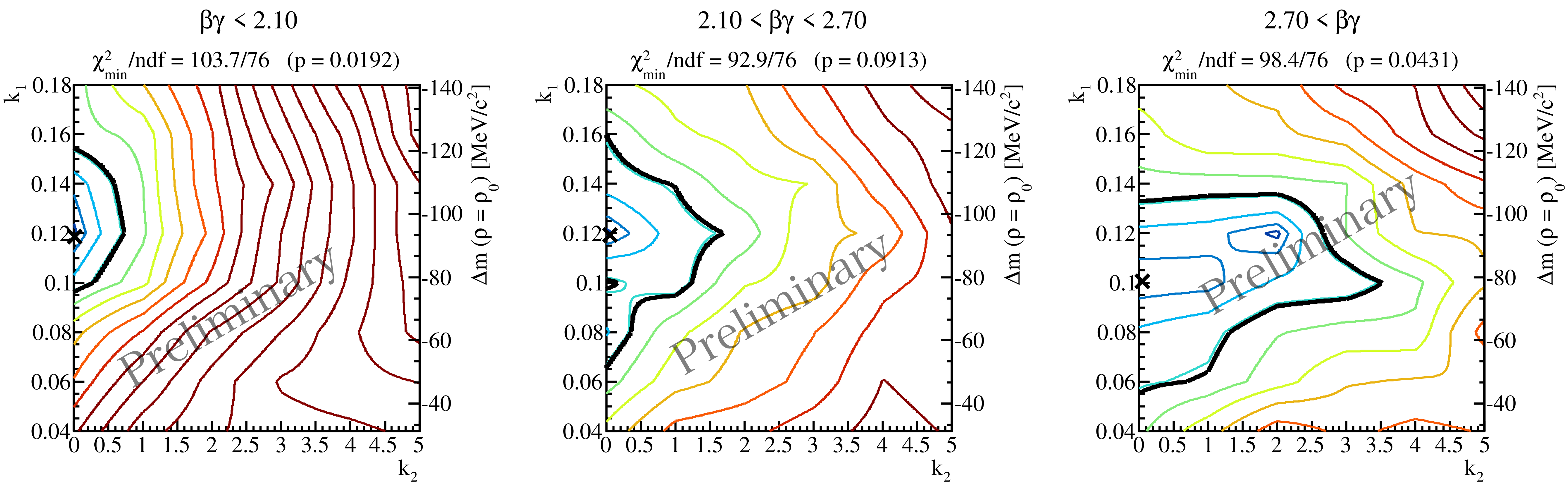

- In case (ii), the optimized k2 values were consistent with 0 (no broadening).
- The optimized k1 values were about 0.10 - 0.12 for all bg regions.
- χ^2 values were better than those of case (i).

Case (ii): nBW/m³

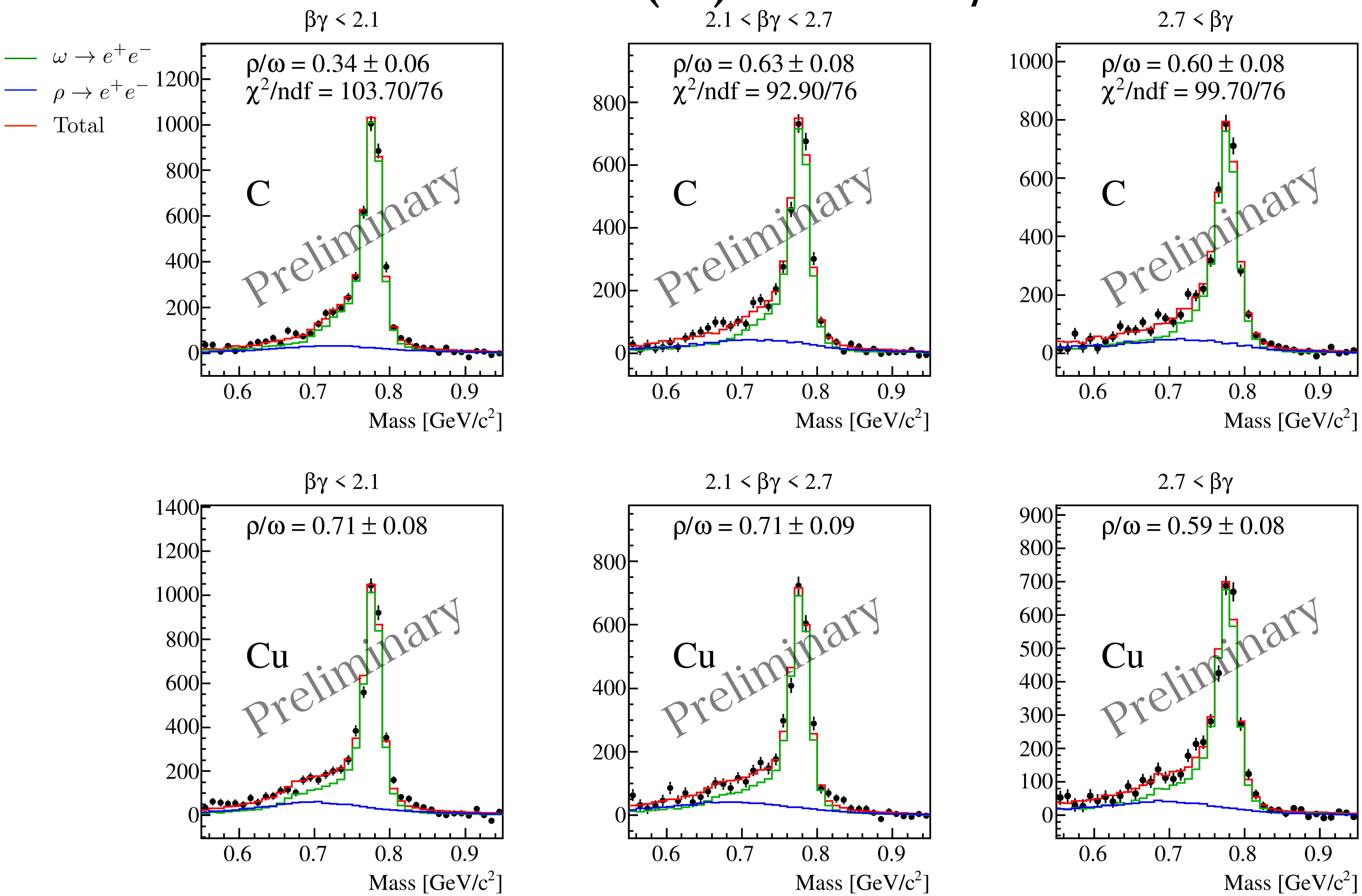

- Since the high mass side of the distribution of ρ is suppressed, the excess can be explained by modified-ρ.

Model fit, Results

		k_1	k_2	ρ/ω (C)	ρ/ω (Cu)	$\chi^2_{\rm min}$/ndf
case (i)	$\beta\gamma < 2.1$	$0.15^{+0.02}_{-0.02}$	$3.3^{+1.0}_{-1.0}$	0.02 ± 0.01	< 0.14	129.3/76
	$2.1 < \beta\gamma < 2.7$	$0.16^{+0.02}_{-0.04}$	$5.9^{+2.6}_{-3.1}$	< 0.18	< 0.01	115.4/76
	$2.7 < \beta\gamma$	$0.12^{+0.05}_{-0.02}$	$5.5^{+3.5}_{-3.6}$	0.25 ± 0.08	< 0.01	122.6/76
case (ii)	$\beta\gamma < 2.1$	$0.12^{+0.03}_{-0.03}$	< 0.7	0.34 ± 0.06	0.71 ± 0.08	103.7/76
	$2.1 < \beta\gamma < 2.7$	$0.12^{+0.04}_{-0.06}$	< 1.7	0.63 ± 0.08	0.71 ± 0.09	92.9/76
	$2.7 < \beta\gamma$	$0.10^{+0.03}_{-0.05}$	< 3.5	0.60 ± 0.08	0.59 ± 0.08	99.7/76

- In the both cases, the k1 parameter had a finite value.
- ρ/ω~0 (case (i)) contradicts a previous p+p result.
- The asymmetric mass shape (case (ii)) reproduces data better than the symmetric one (case (i)).

k1 vs momentum (case (ii))

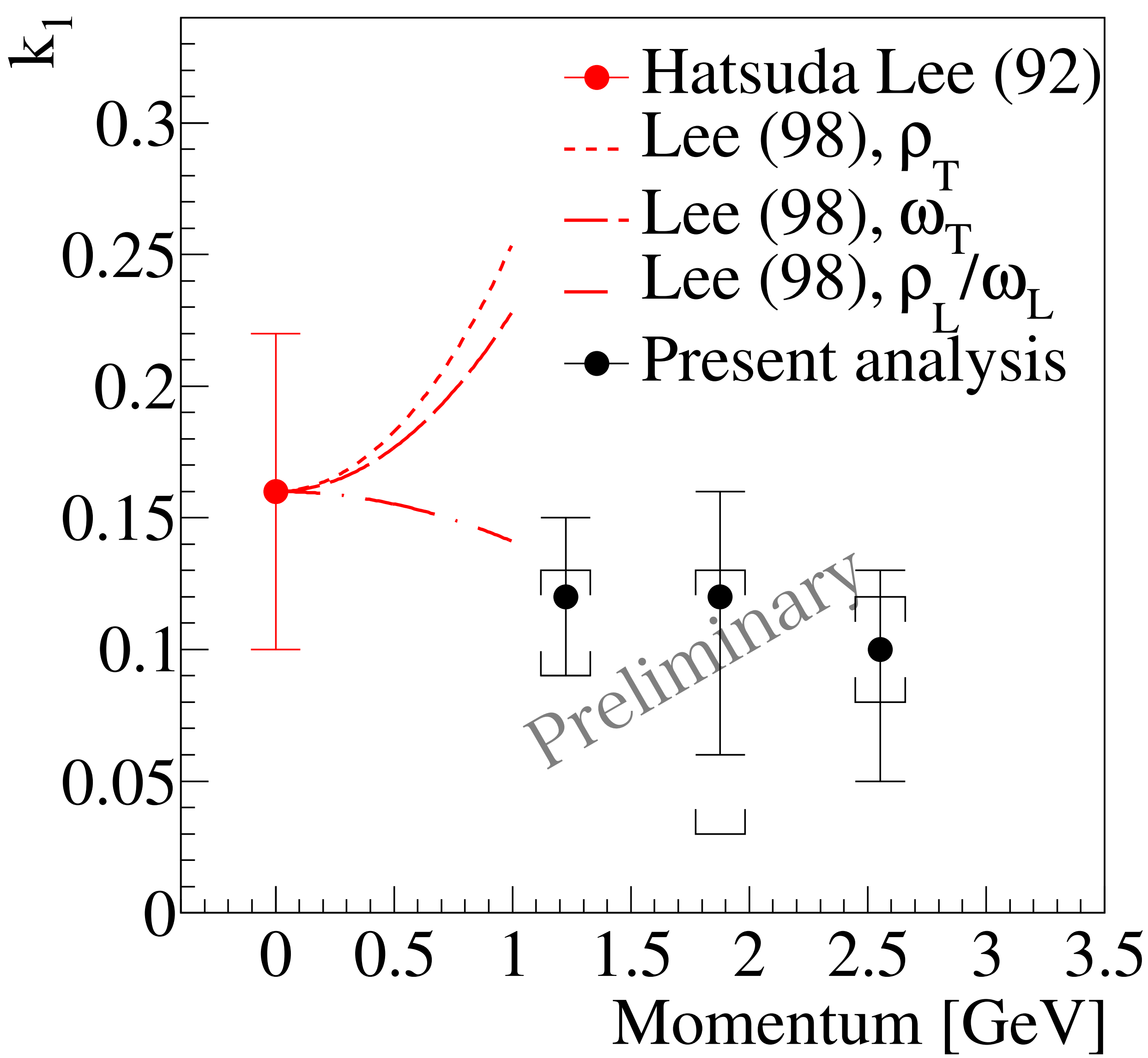

- Conclusions
  - k1 > 0 in any region, and the values are consistent with Hatsuda-Lee's value.
  - Momentum dependence is not significant.
  - The results can not be compared with S.H. Lee's calculation because the momentum region is p < 1 GeV/c.
    - However, it is consistent with the results of longitudinal.

Summary

- Re-analysis of the E325 data was performed.
  - Statistics improved by a factor of three from the previous analysis.
- Significant excesses were observed for all targets and all $\beta\gamma$ regions.
- Some model calculations were performed to evaluate the mass modification of ρ and ω mesons.
  - k1 > 0 for all regions, and the values are consistent with Hatsuda-Lee's value.
  - Asymmetric distribution reproduces the data better than when using symmetric distribution.
  - In case (ii), the result about k2 was consistent with no broadening.

Backups

KEK-PS E325 experiment

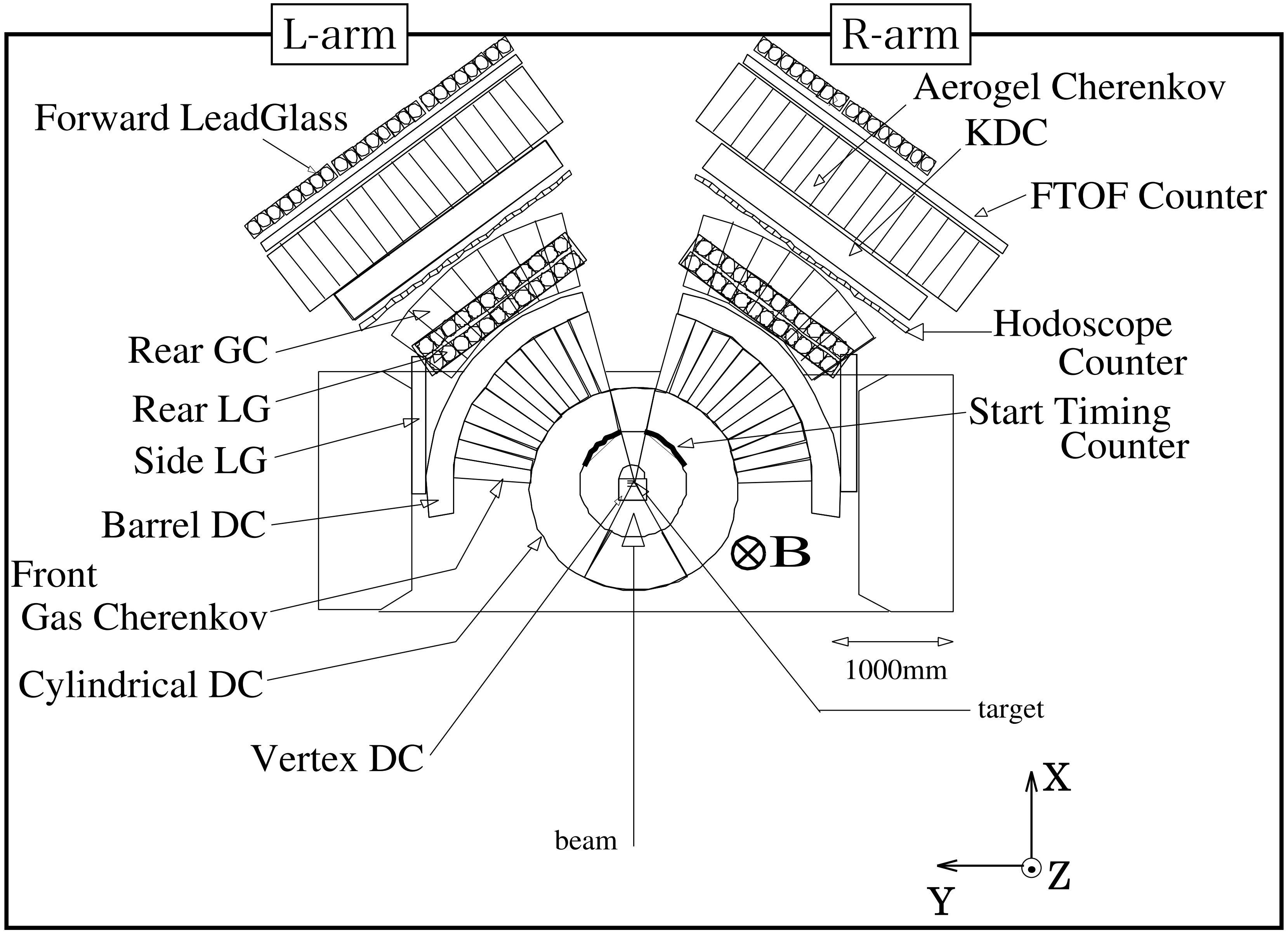

- Tracking : Cylindrical Drift Chamber (CDC), Barrel DC (BDC)
- EID : Front Gas Cherenkov (FGC), Rear GC (RGC), Forward Lead Glass calorimeter (FLG), Real LG (RLG), Side LG (SLG)
- Start Timing Counter (STC)

Target

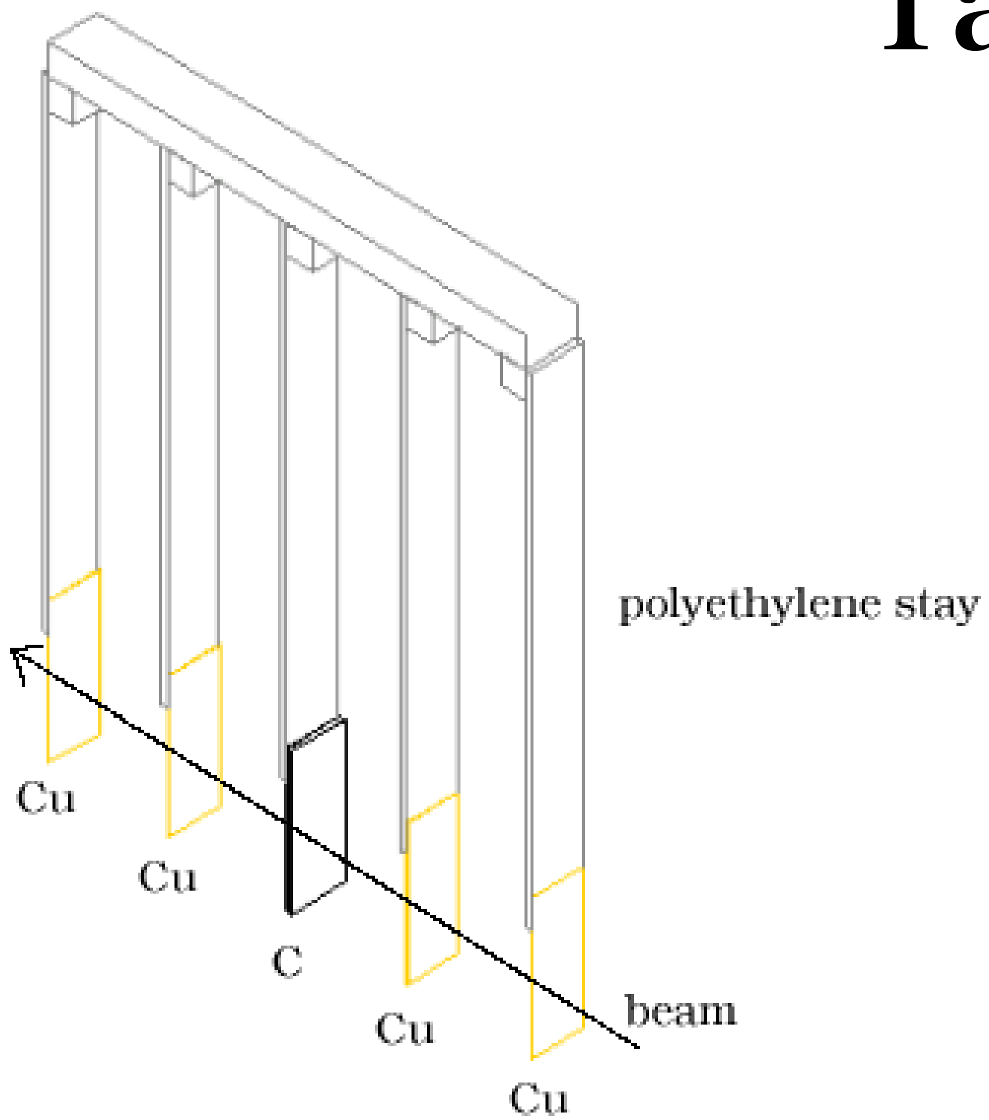

- Several thin targets are placed along the beam axis.
- The year 2001: one C + two Cu
- The year 2002: one C + four Cu (Left picture)
- Take the data simultaneously and reconstruct the reaction points by offline analysis.

material	mass number	x position [mm]	width [mm]	height [mm]	thickness [mg/cm^2]	interaction length [%]	radiation length [%]
			2001				
carbon	12.011	0	25	25	92	0.11	0.21
copper	63.546	± 48	25	25	2×73	2×0.054	2×0.57
			2002				
carbon	12.011	0	10	25	184	0.21	0.43
copper	63.546	$-43, -23, +24, +48$	10	25	4×73	4×0.054	4×0.57

Table 2.3: Configuration of the targets used in the year 2001 and 2002.

Target selection

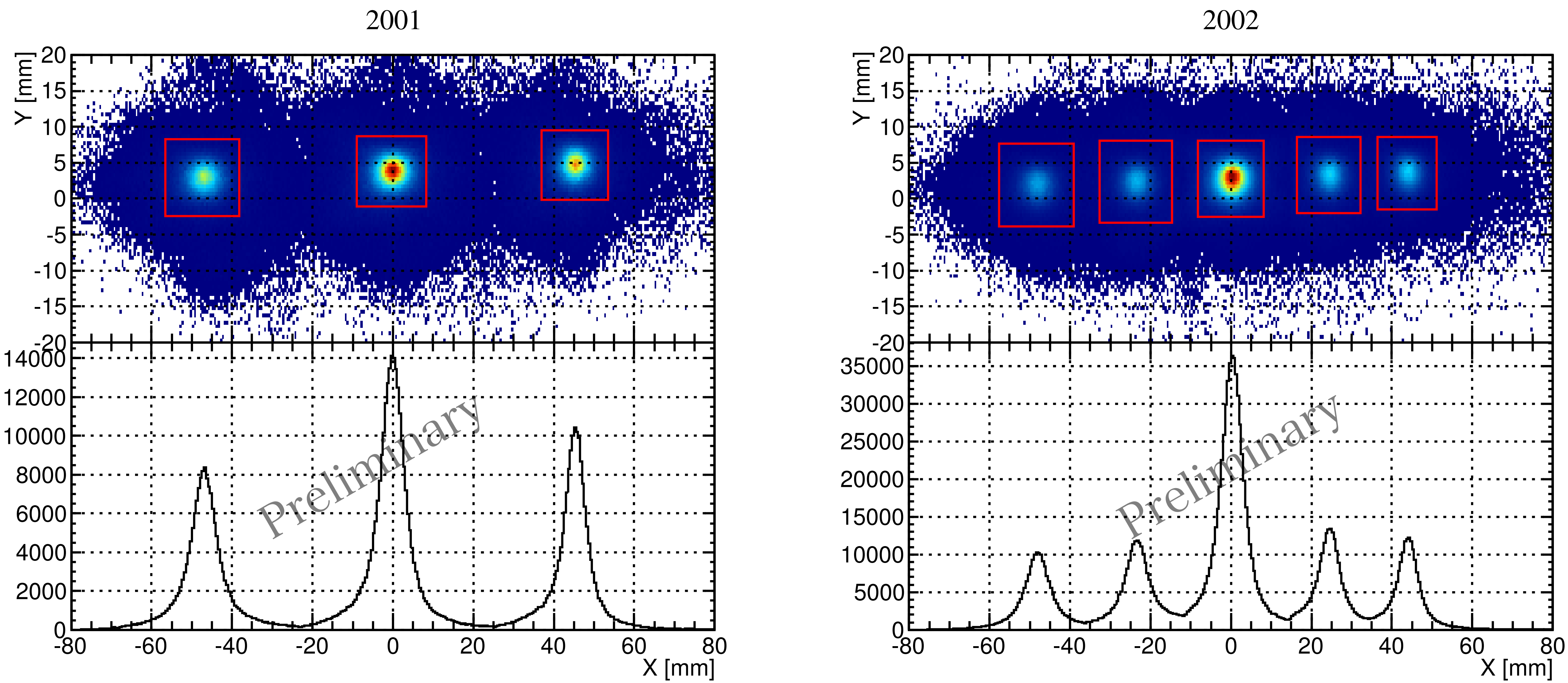

- The vertex position was determined as the nearest point from all tracks of the same event.
- Cut within $\pm 3\sigma$ of peak position (each axis)

Obtained mass spectra

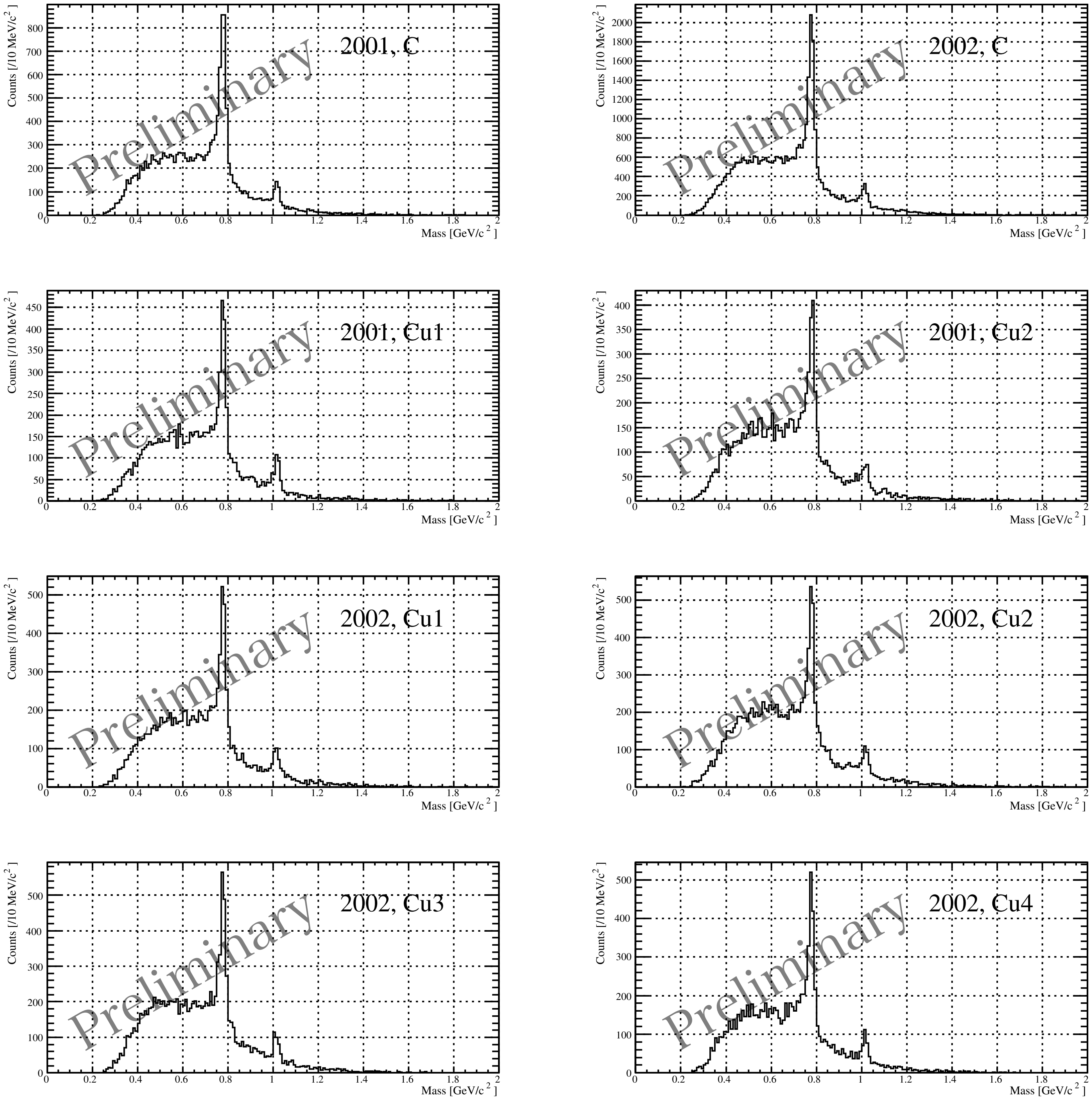

- For each dataset, each target position.
- Target position dependence was reduced by the fiducial cut.
- Clear ω and ϕ peaks can be observed.

Excess ratio, Systematic error

- Fit条件を変えながらexcess ratioを求め、系統誤差を評価

- A : Fit範囲を変える
- B : Massのbin幅を変える
- C : Mass scaleを変える
- D : Mass smearを変える
- E : Event mixing法を変える

- 各カテゴリーで一番大きいものを2乗和する

Carbon			
Condition	$\beta\gamma < 2.1$	$2.1 < \beta\gamma < 2.7$	$2.7 < \beta\gamma$
A1	1.1 %	6.9 %	7.9 %
A2	7.2 %	9.3 %	12.8 %
B1	13.8 %	10.3 %	16.0 %
B2	3.2 %	1.4 %	10.5 %
C1	7.1 %	7.3 %	12.2 %
C2	9.3 %	8.5 %	13.3 %
D1	3.4 %	0.5 %	0.8 %
D2	5.0 %	6.2 %	3.7 %
E1	2.6 %	1.7 %	2.6 %
E2	7.9 %	5.9 %	5.0 %
E3	1.5 %	0.6 %	2.5 %
Total	20.4 %	18.4 %	25.2 %

Copper			
Condition	$\beta\gamma < 2.1$	$2.1 < \beta\gamma < 2.7$	$2.7 < \beta\gamma$
A1	2.1 %	9.0 %	10.3 %
A2	4.7 %	7.4 %	8.8 %
B1	7.0 %	9.0 %	13.1 %
B2	2.0 %	5.4 %	4.1 %
C1	4.3 %	6.3 %	7.1 %
C2	5.2 %	5.9 %	7.0 %
D1	2.1 %	0.2 %	1.2 %
D2	3.0 %	4.0 %	3.5 %
E1	2.0 %	1.8 %	1.1 %
E2	5.9 %	6.0 %	2.8 %
E3	2.4 %	0.1 %	2.0 %
Total	11.9 %	16.0 %	18.7 %

Mass shape formulae

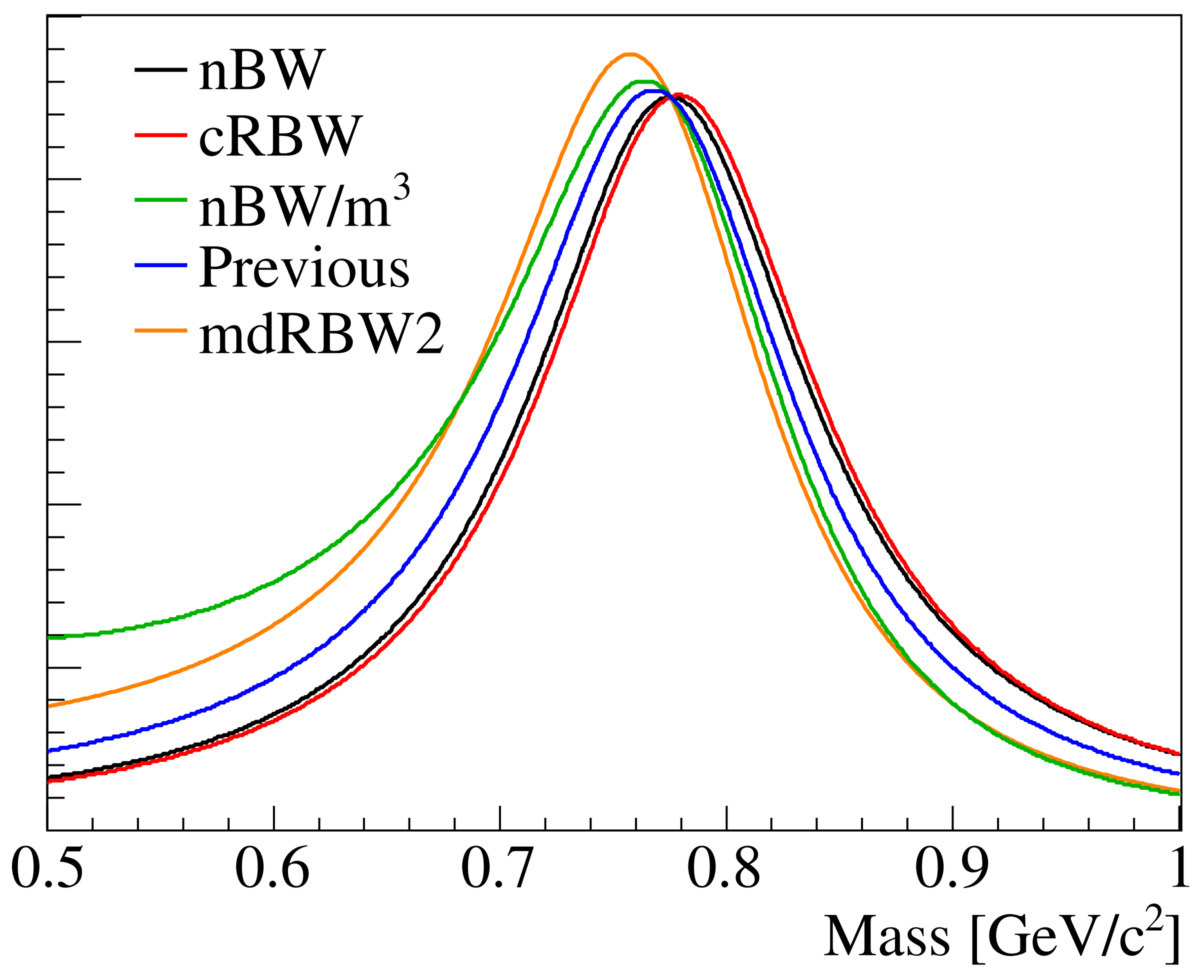

non-relativistic Breit-Wigner

$$\mathrm{nBW}(m) = \frac{\Gamma_{\mathrm{tot}}}{2\pi} \frac{1}{(m-m_0)^2 + \Gamma_{\mathrm{tot}}^2/4},$$

constant-width Relativistic Breit-Wigner

$$\mathrm{cRBW}(m) = \frac{2}{\pi} \frac{m m_0 \Gamma_{ee}}{(m^2-m_0^2)^2 + m_0^2\Gamma_{\mathrm{tot}}^2},$$

mass-dependent-width Relativistic Breit-Wigner

$$\mathrm{mdRBW}(m) = \frac{2}{\pi} \frac{m^2 \Gamma_{ee}(m)}{(m^2-m_0^2)^2 + m^2\Gamma_{\mathrm{tot}}(m)^2},$$

mdRBW and assuming $\varGamma_{\mathrm{tot}}(m) = \frac{m}{m_0}\varGamma_{\mathrm{tot}}$

$$\varGamma_{ee}(m) = \left(\frac{m_0}{m}\right)^3 \varGamma_{ee}$$

$$\mathrm{mdRBW2}(m) = \frac{2}{\pi} \frac{(m_0^3/m)\Gamma_{ee}}{(m^2-m_0^2)^2 + (m^4/m_0^2)\Gamma_{\mathrm{tot}}^2}$$

case (iii): nBW + unmodified omega

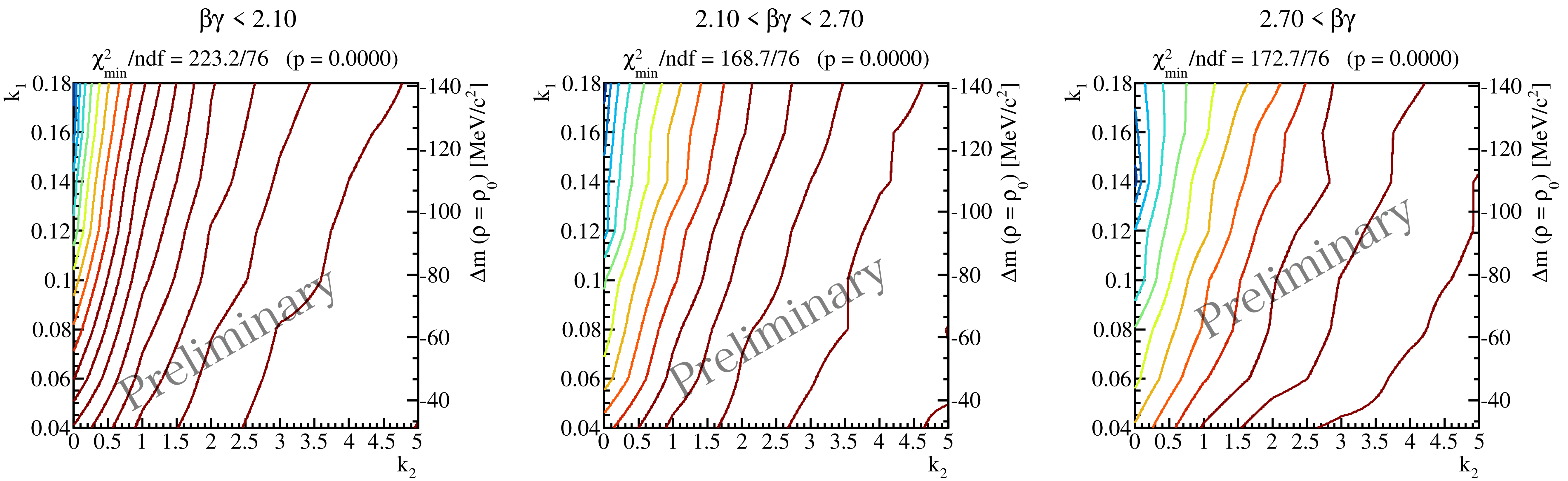

- Fixed the mass shape of ω meson vacuum one.
- Only the modification of ρ meson was allowed.

Case (iii) : nBW + unmodified omega

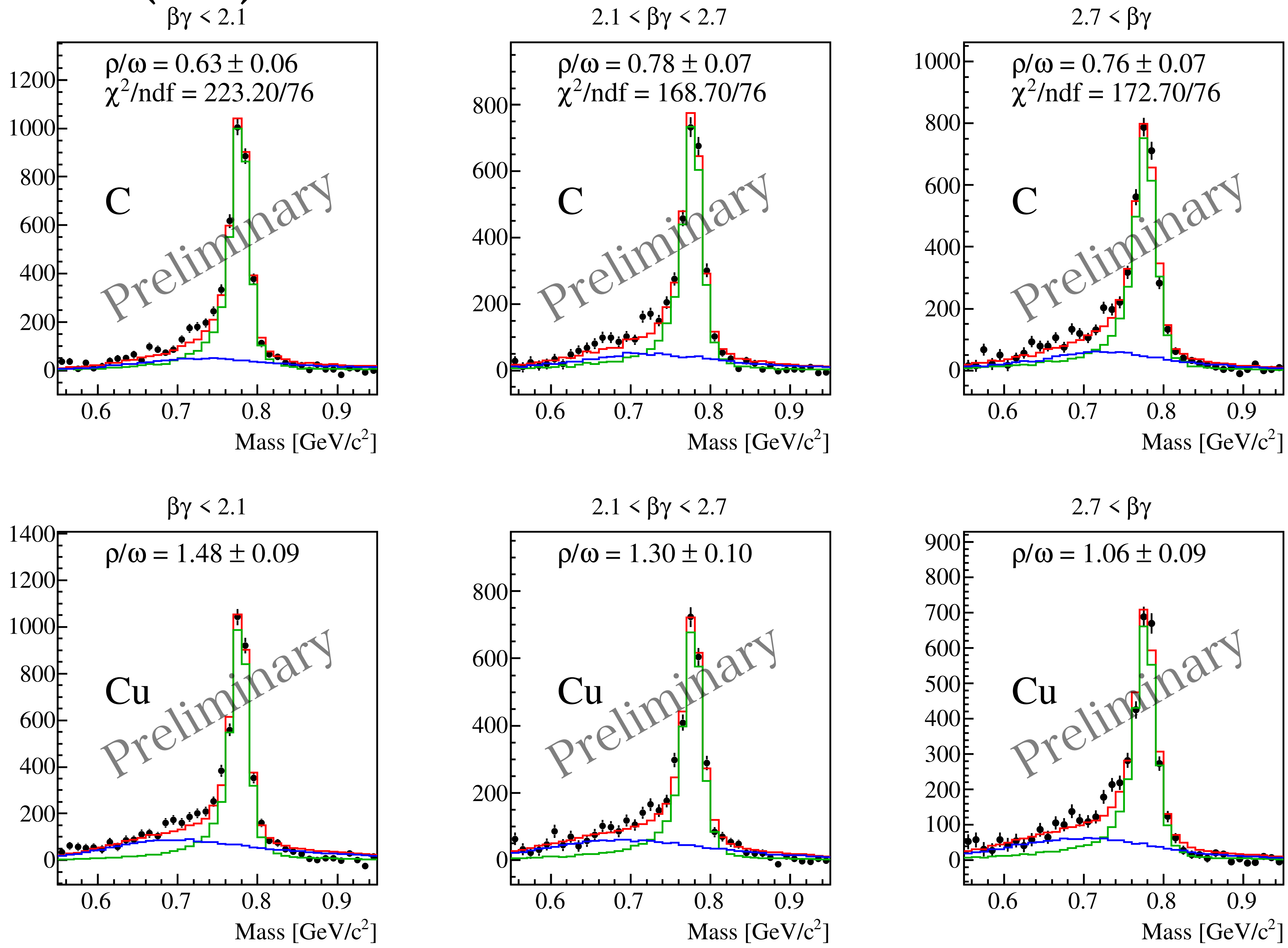

Case (iv) : nBW/m^3 + unmodified omega

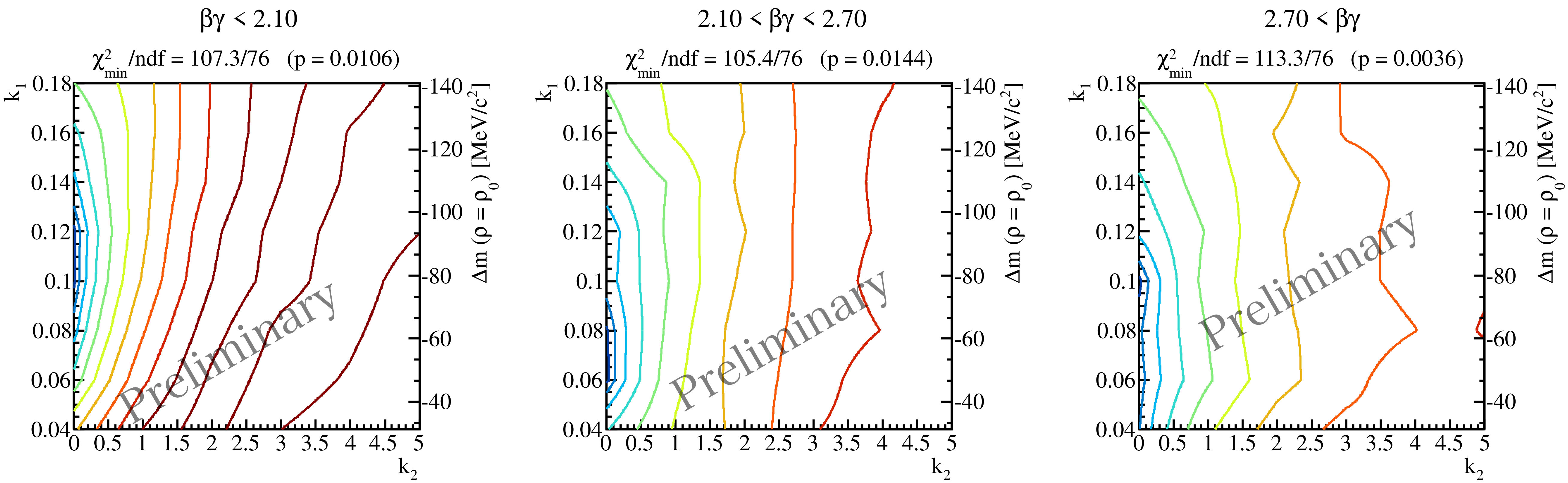

Case (iv) : nBW/m^3 + unmodified omega

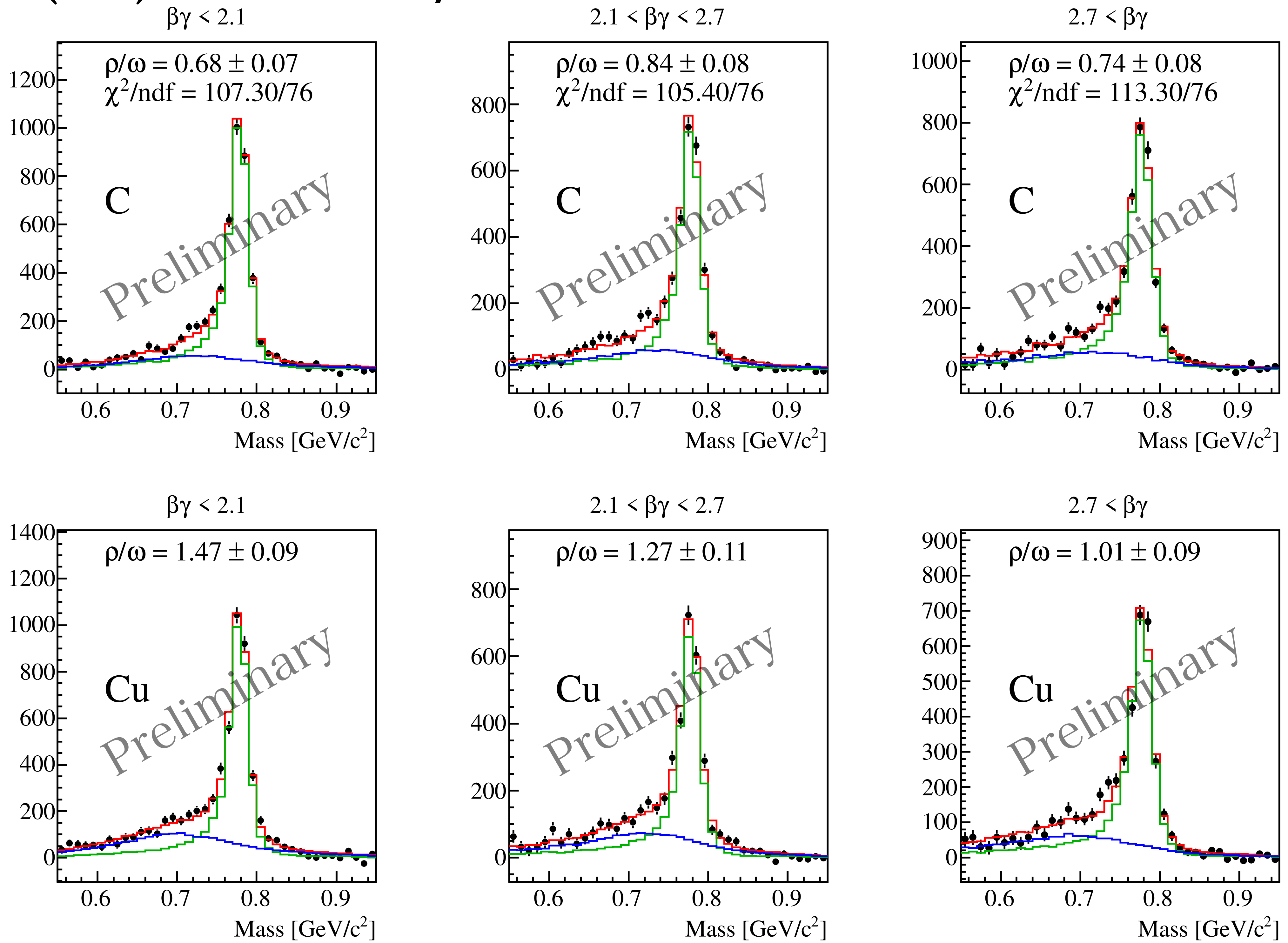

Model fit, Results

		k_1	k_2	ρ/ω (C)	ρ/ω (Cu)	$\chi^2_{min}/\mathrm{ndf}$	
case (i)	$\beta\gamma < 2.1$	$0.15^{+0.02}_{-0.02}$	$3.3^{+1.0}_{-1.0}$	0.02 ± 0.01	< 0.14	129.3/76	
	$2.1 < \beta\gamma < 2.7$	$0.16^{+0.02}_{-0.04}$	$5.9^{+2.6}_{-3.1}$	< 0.18 ×	< 0.01	115.4/76	
	$2.7 < \beta\gamma$	$0.12^{+0.05}_{-0.02}$	$5.5^{+3.5}_{-3.6}$	0.25 ± 0.08	< 0.01	122.6/76	
case (ii)	$\beta\gamma < 2.1$	$0.12^{+0.03}_{-0.03}$	< 0.7	0.34 ± 0.06	0.71 ± 0.08	103.7/76	
	$2.1 < \beta\gamma < 2.7$	$0.12^{+0.04}_{-0.06}$	< 1.7	0.63 ± 0.08	0.71 ± 0.09	92.9/76	◎
	$2.7 < \beta\gamma$	$0.10^{+0.03}_{-0.05}$	< 3.5	0.60 ± 0.08	0.59 ± 0.08	99.7/76	
case (iii)	$\beta\gamma < 2.1$	$0.14^{+0.04}_{-0.02}$	< 0.2	0.63 ± 0.06	1.48 ± 0.09	223.2/76	
	$2.1 < \beta\gamma < 2.7$	$0.15^{+0.03}_{-0.05}$	< 0.4	0.78 ± 0.07	1.30 ± 0.10	168.7/76	×
	$2.7 < \beta\gamma$	$0.15^{+0.04}_{-0.05}$	< 0.5	0.76 ± 0.07	1.06 ± 0.09	172.7/76	
case (iv)	$\beta\gamma < 2.1$	$0.11^{+0.05}_{-0.05}$	< 0.4	0.68 ± 0.07	1.47 ± 0.09	107.3/76	
	$2.1 < \beta\gamma < 2.7$	$0.07^{+0.08}_{-0.03}$	< 0.6	0.84 ± 0.08	1.27 ± 0.11	105.4/76	○
	$2.7 < \beta\gamma$	$0.09^{+0.05}_{-0.05}$	< 0.7	0.74 ± 0.08	1.01 ± 0.09	113.3/76	

- Representative values of k1 and k2 are obtained by fitting a parabolic surface around the grid point to minimize.
- Statistical errors and upper bounds for k1 and k2 were obtained from $\Delta\chi^2 = 16.81$
- ρ/ω~0 case (i) contradicts the p+p result.
- case (ii) is the best. The difference from case (iv) is less than 16.81.

Excluding the excess region

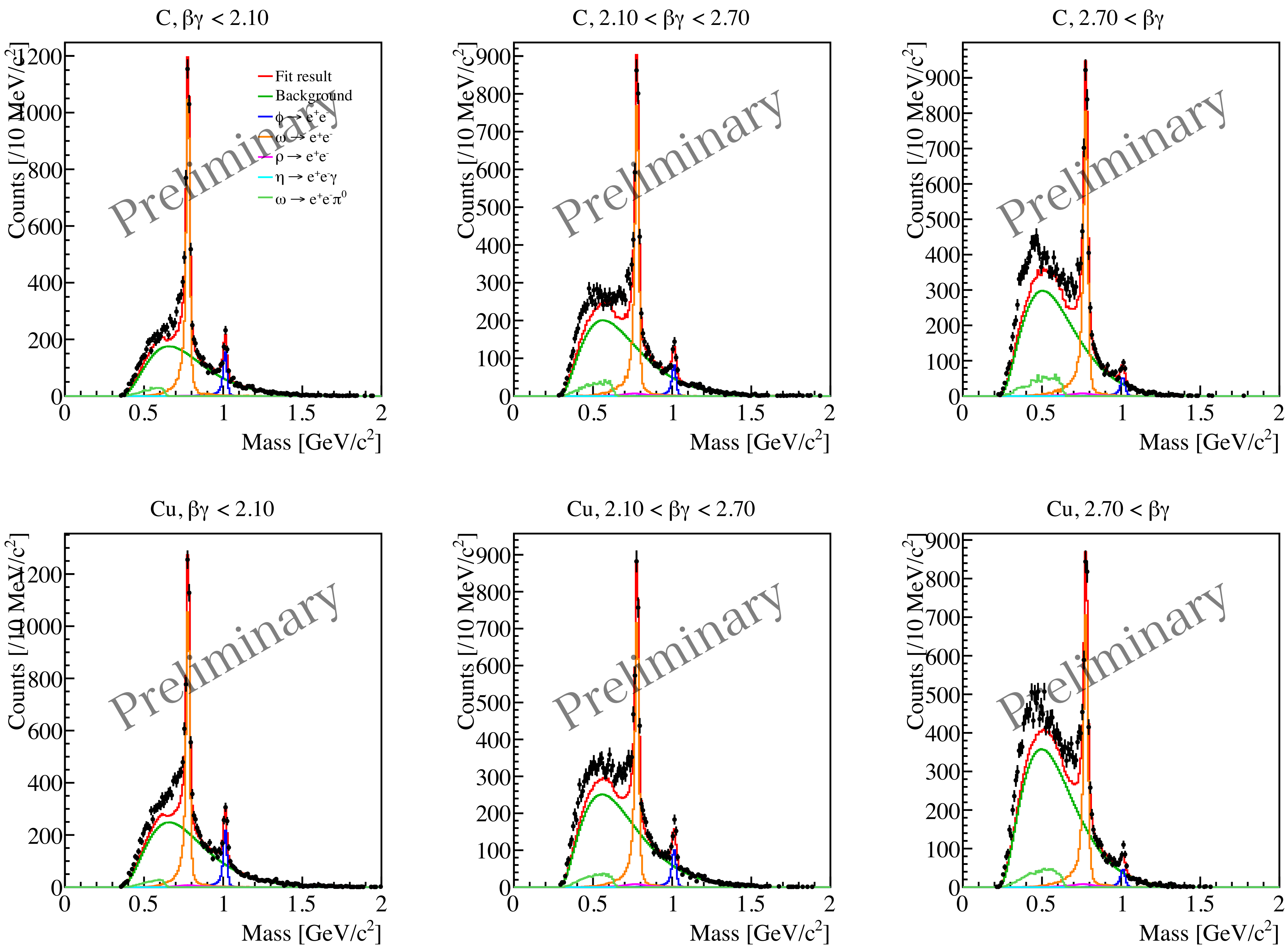

Excluding the excess region, including η

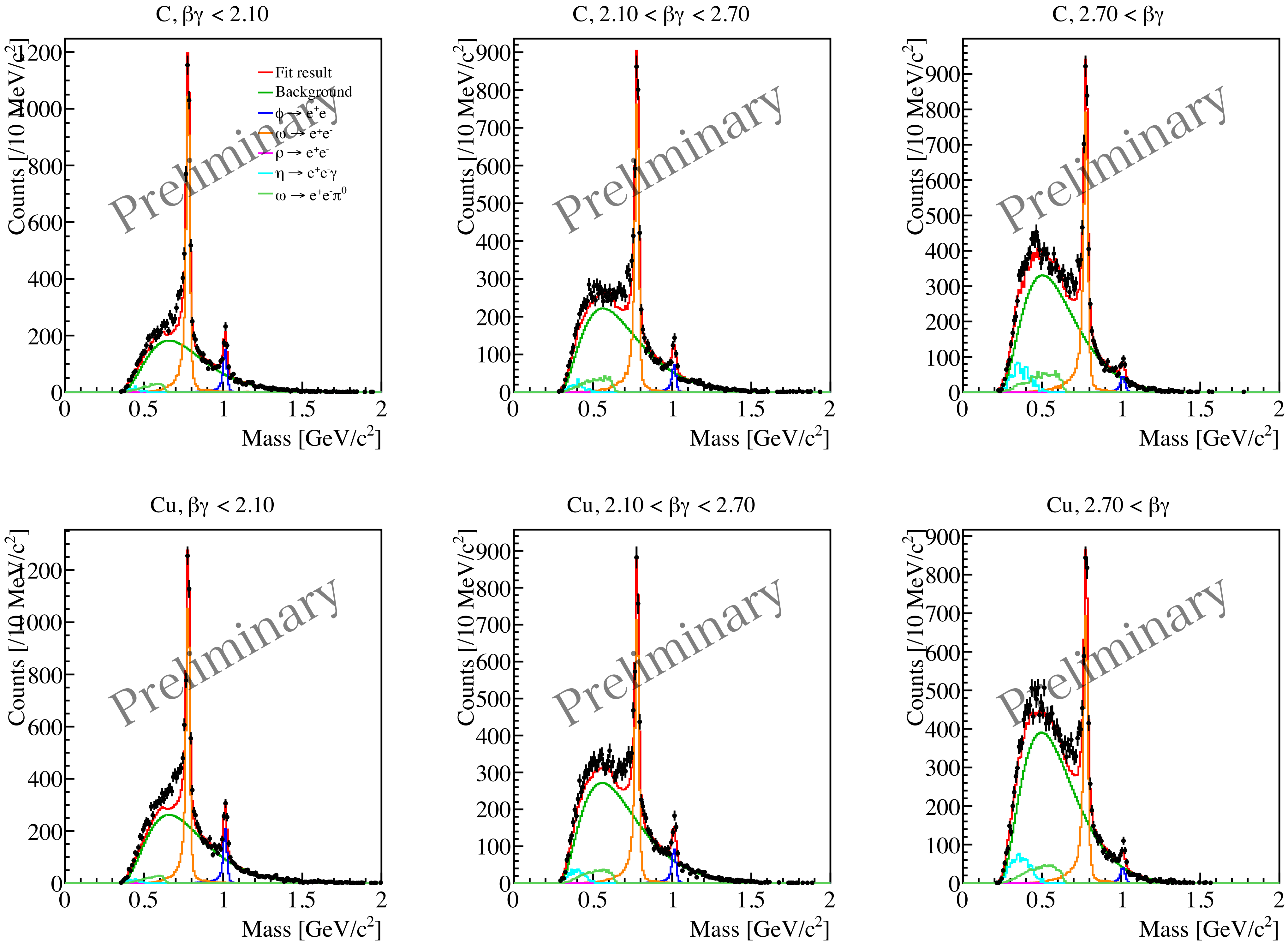

Including the excess region

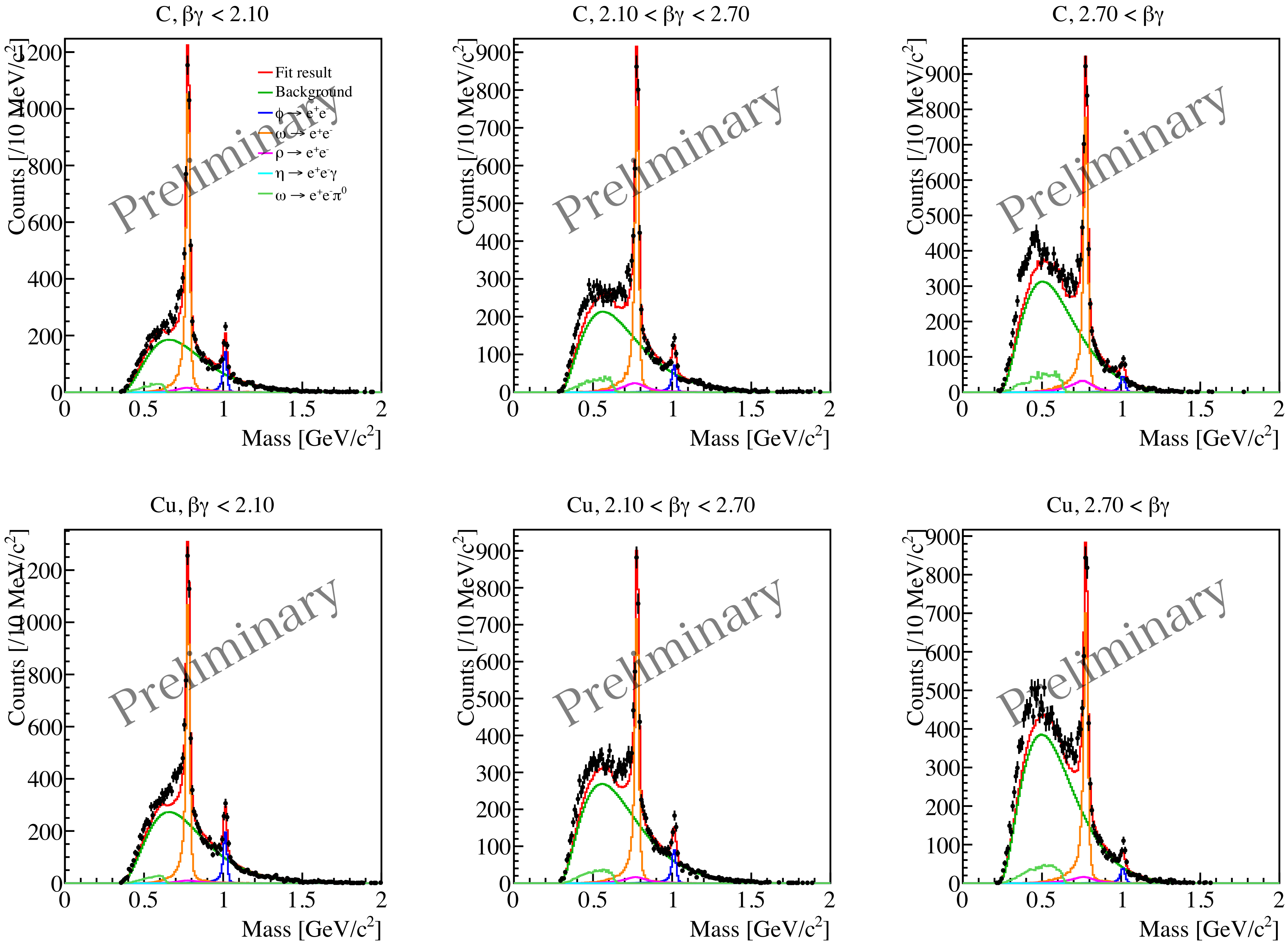

Including the excess region, including η

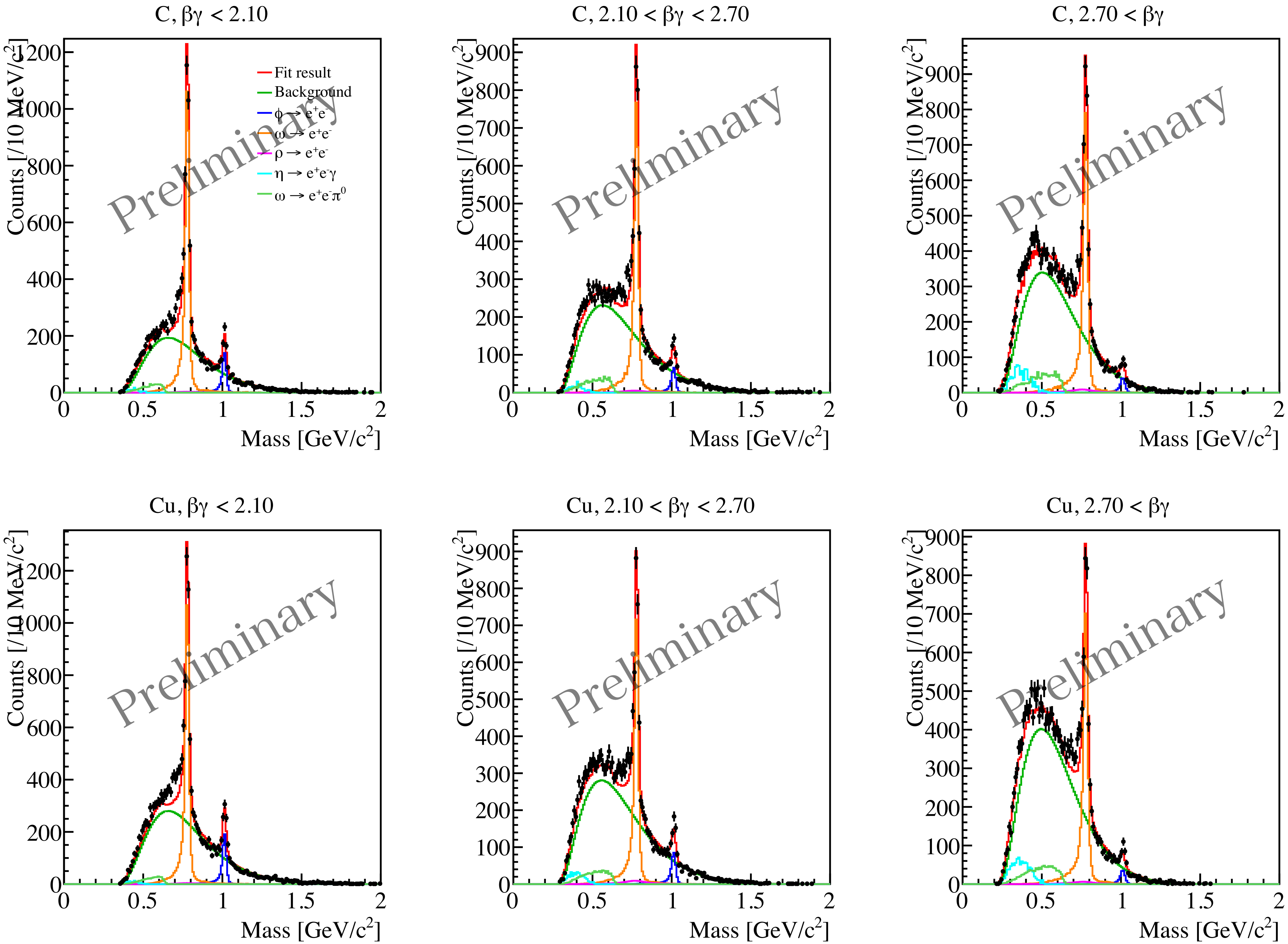

Excluding the excess region

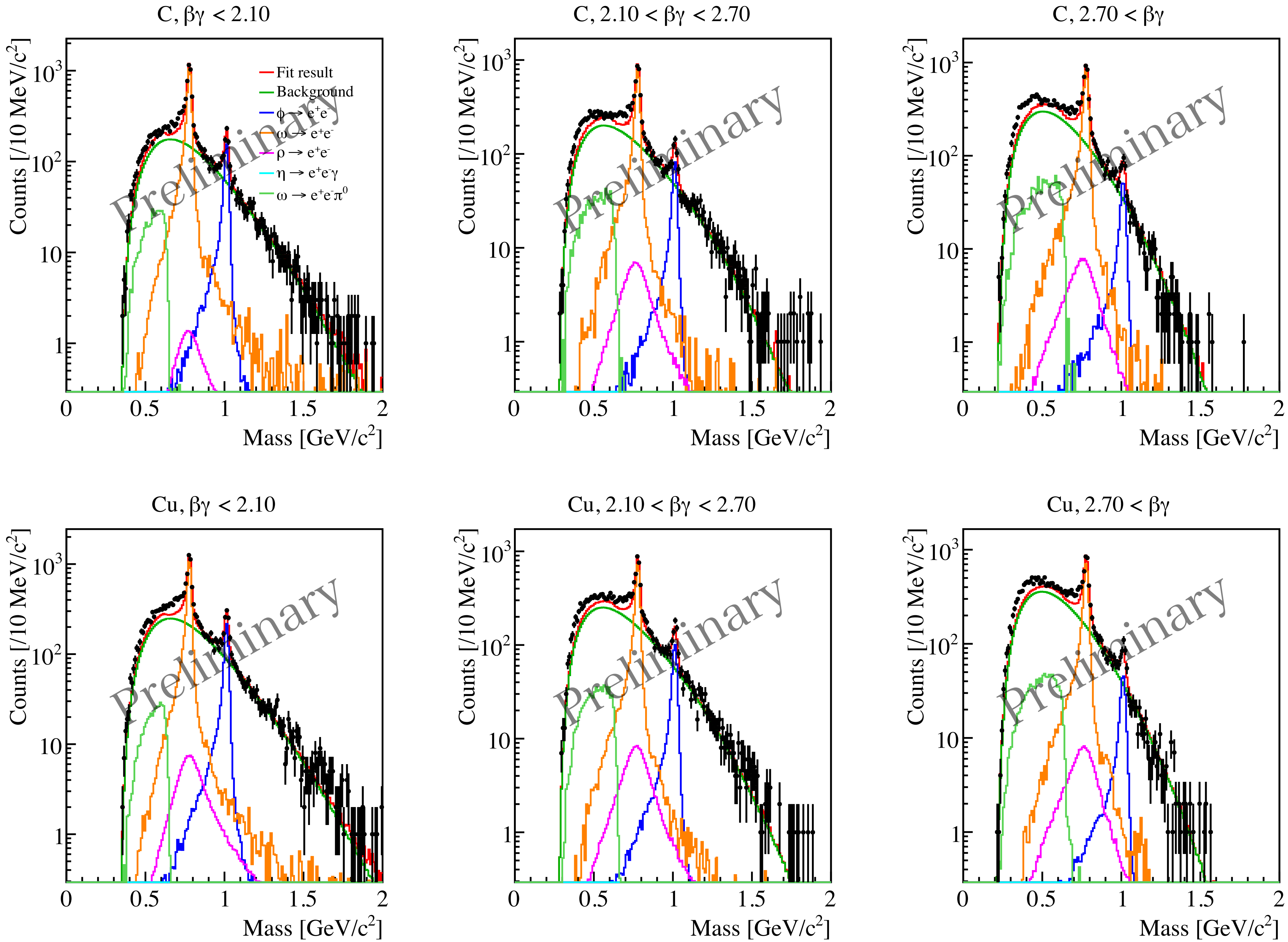

Excluding the excess region, including η

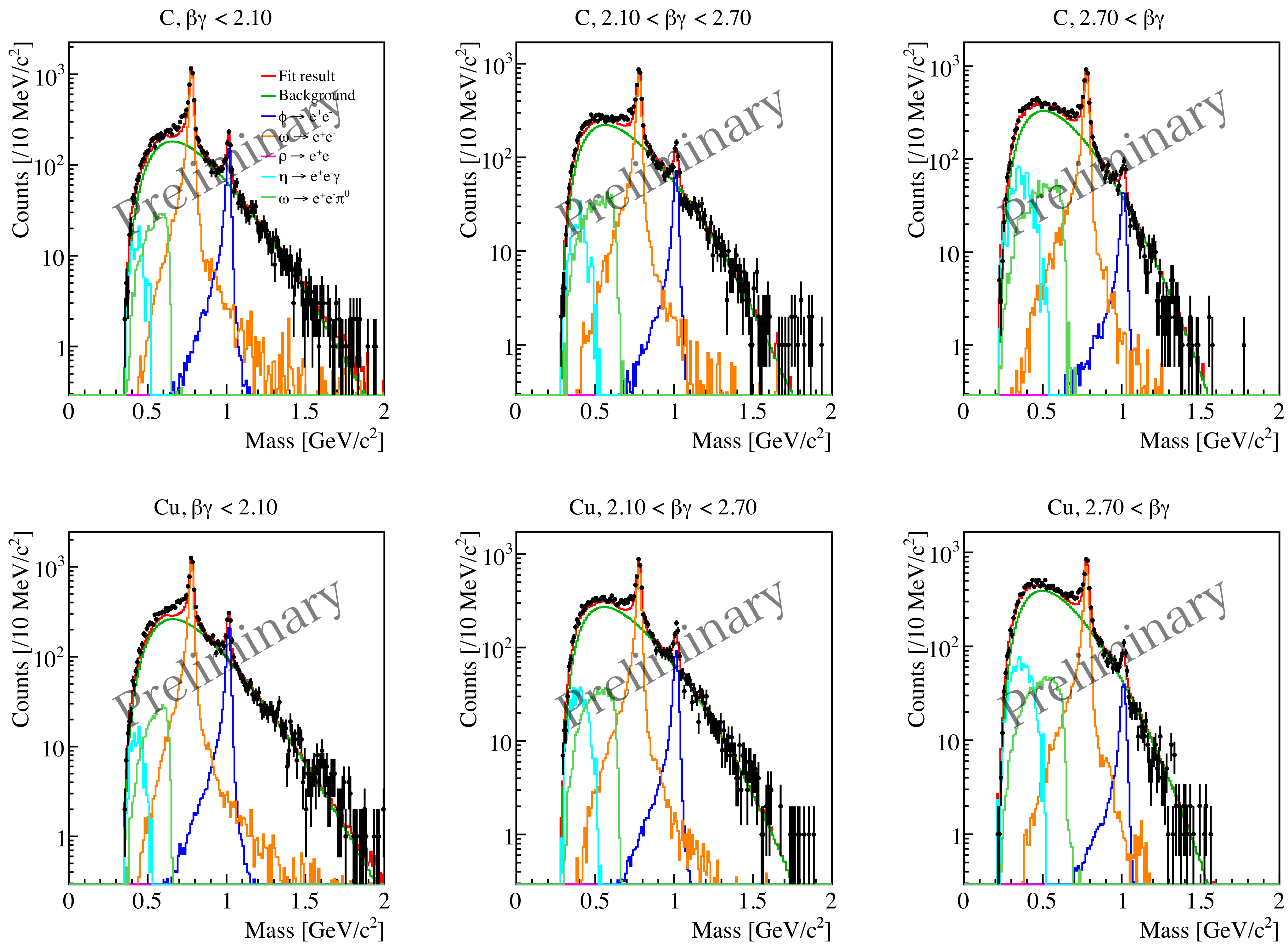

Including the excess region

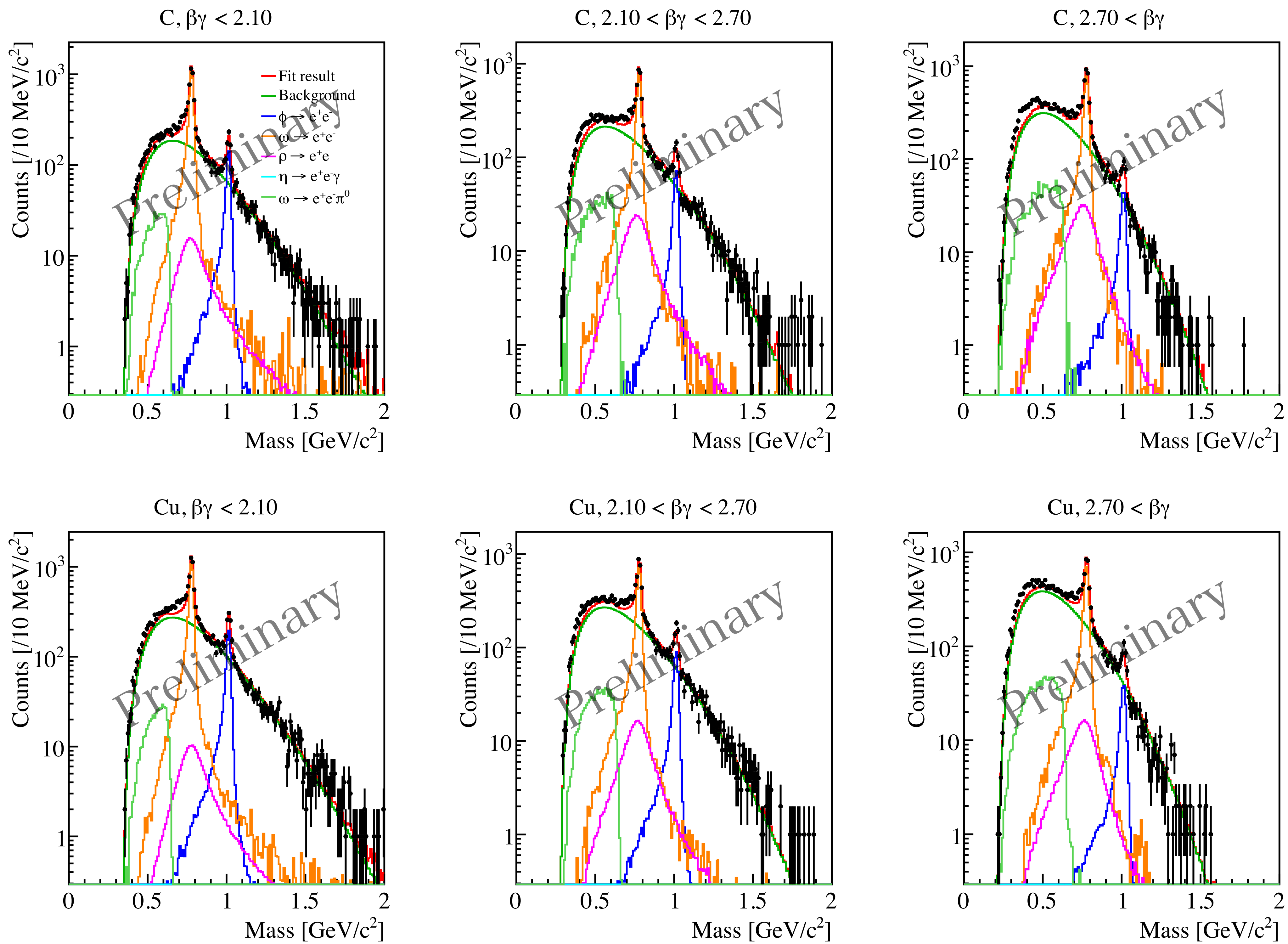

Including the excess region, including η

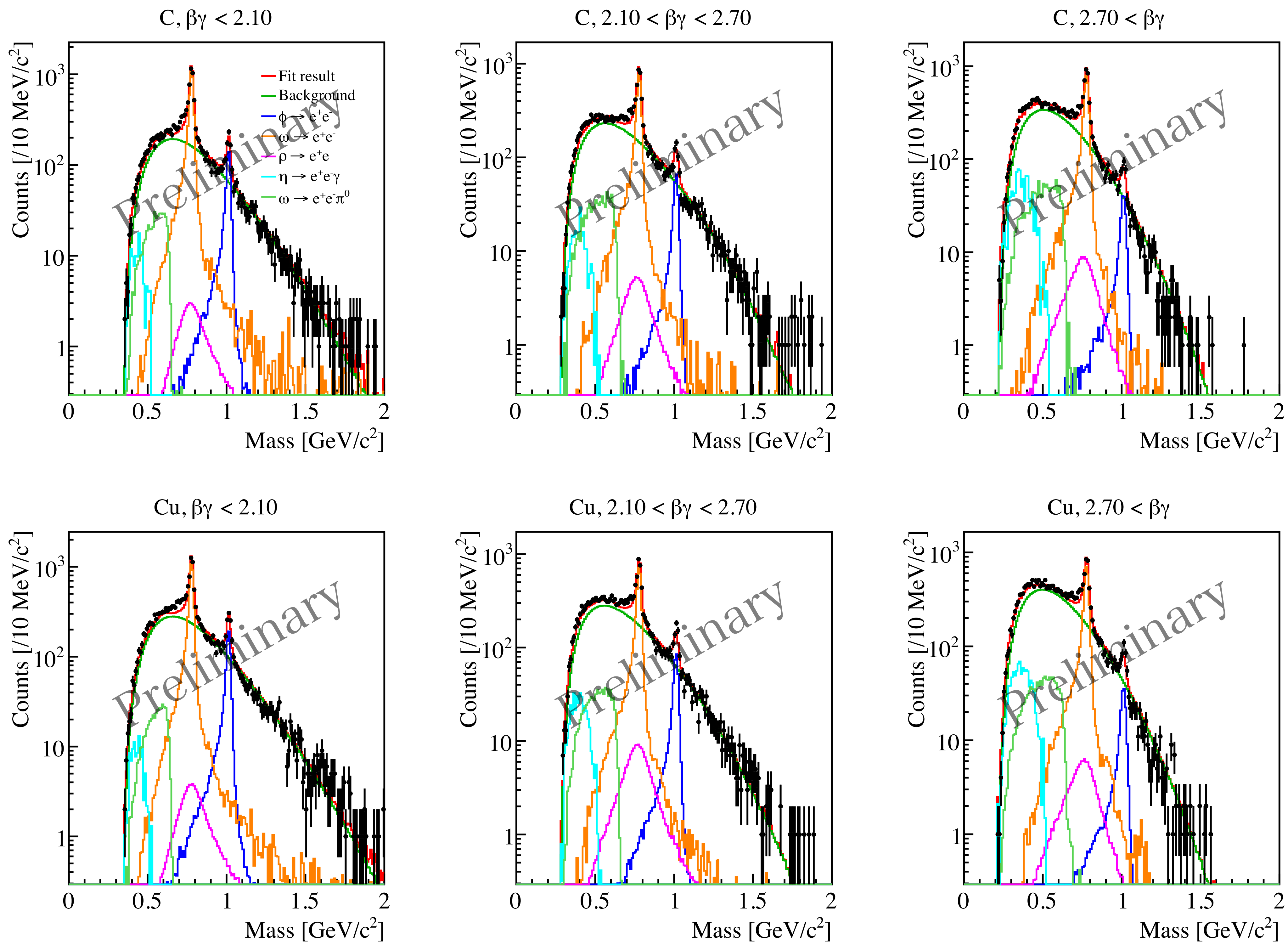

θ_CM distribution (Helicity angle of ω->ee) extracted by Side band subtraction method

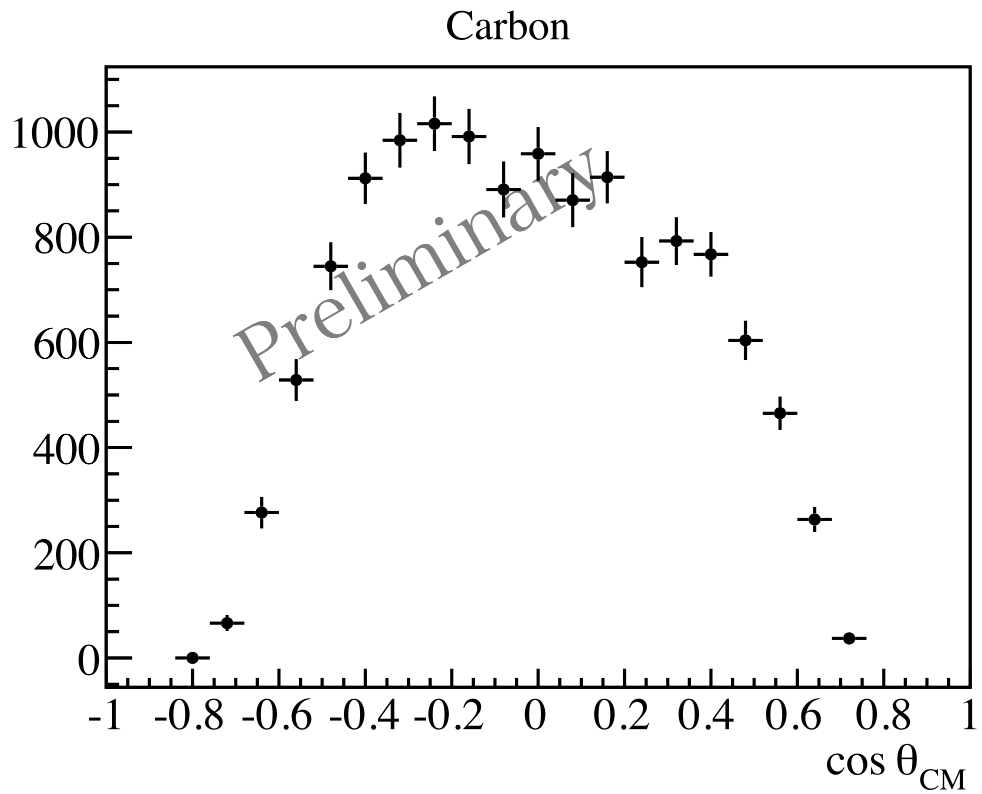

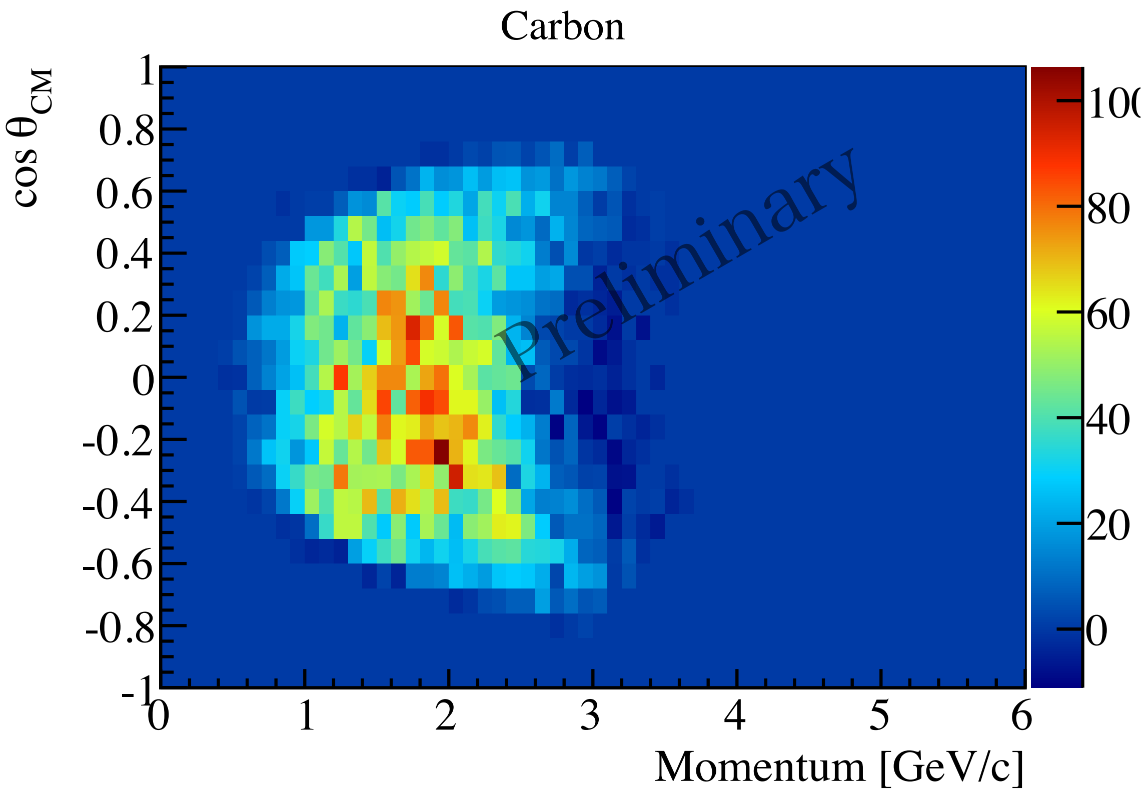

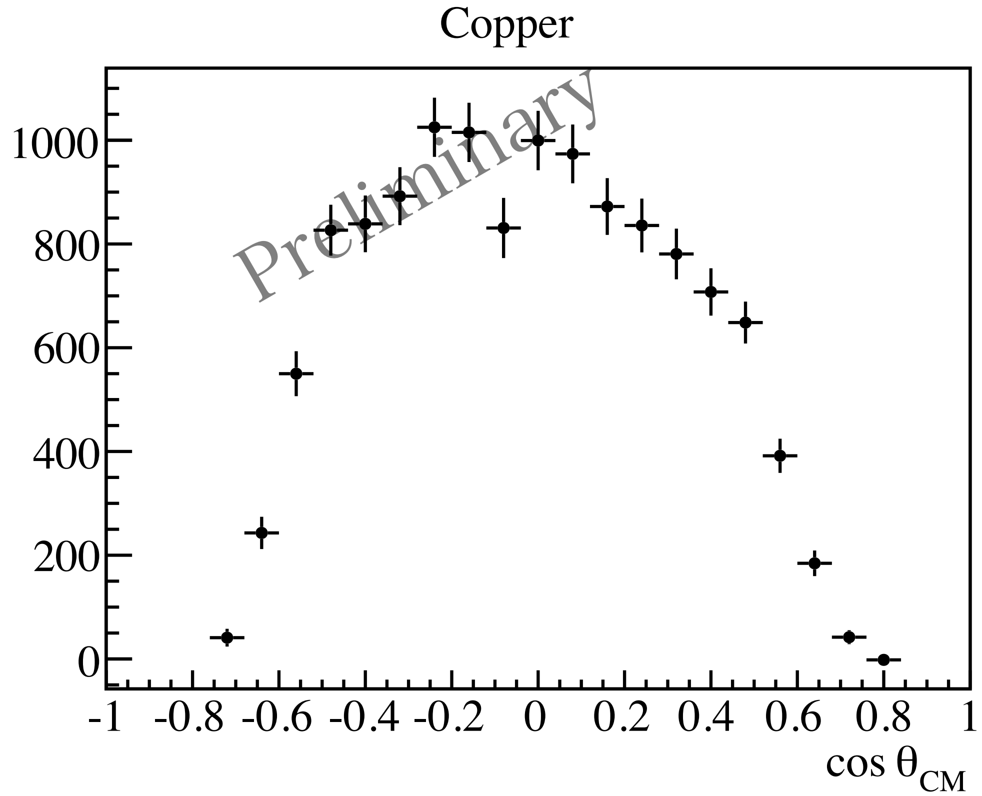

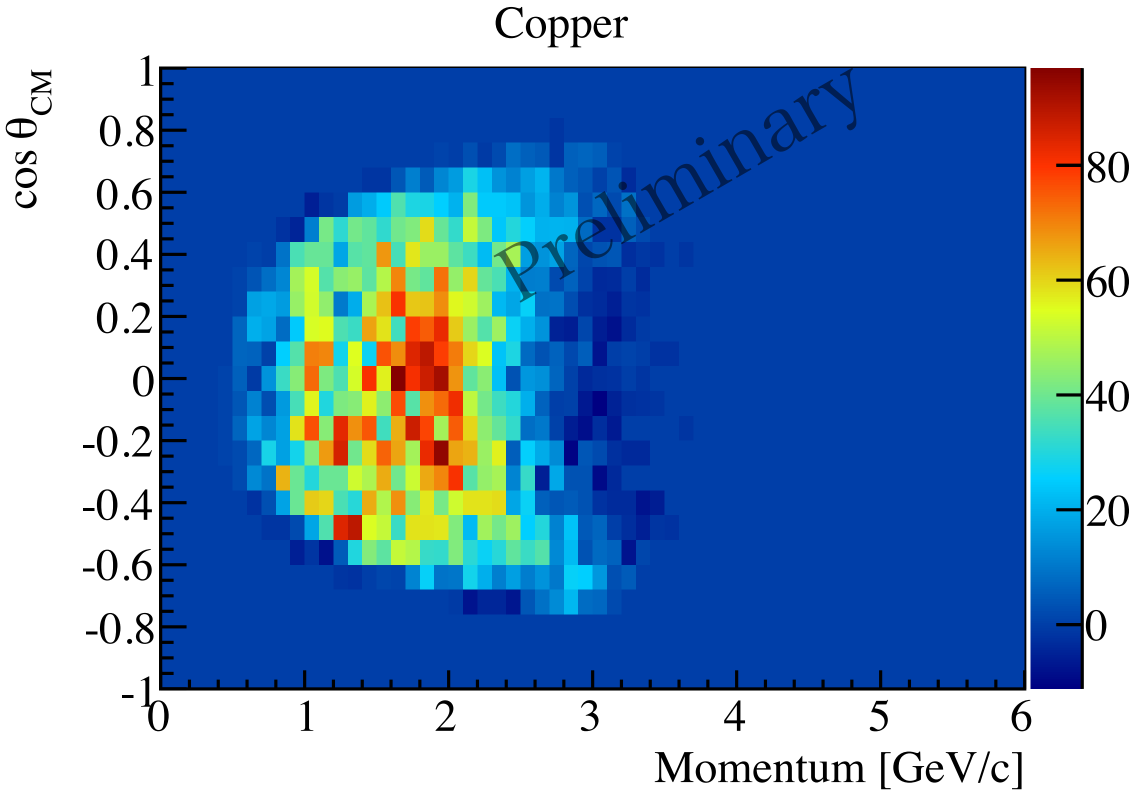

rho0 -> ee, after Vertex momentum cut

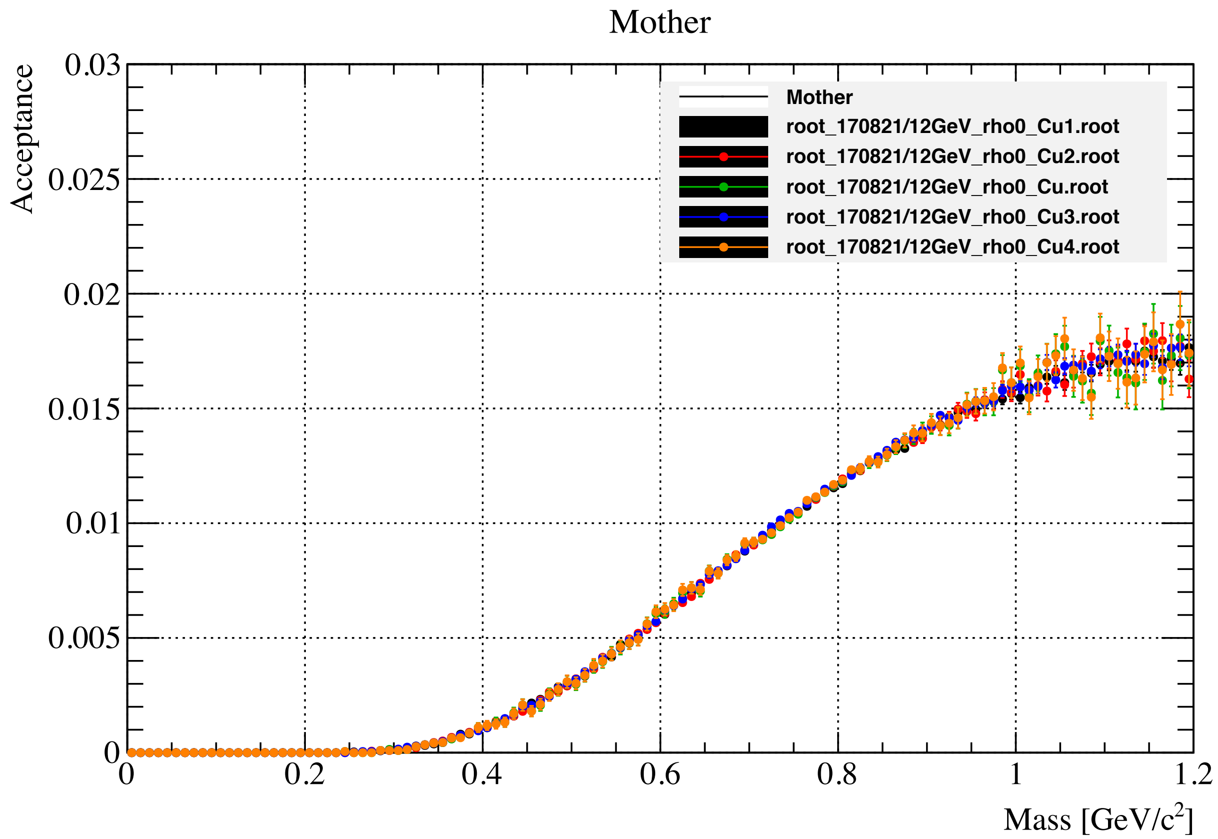

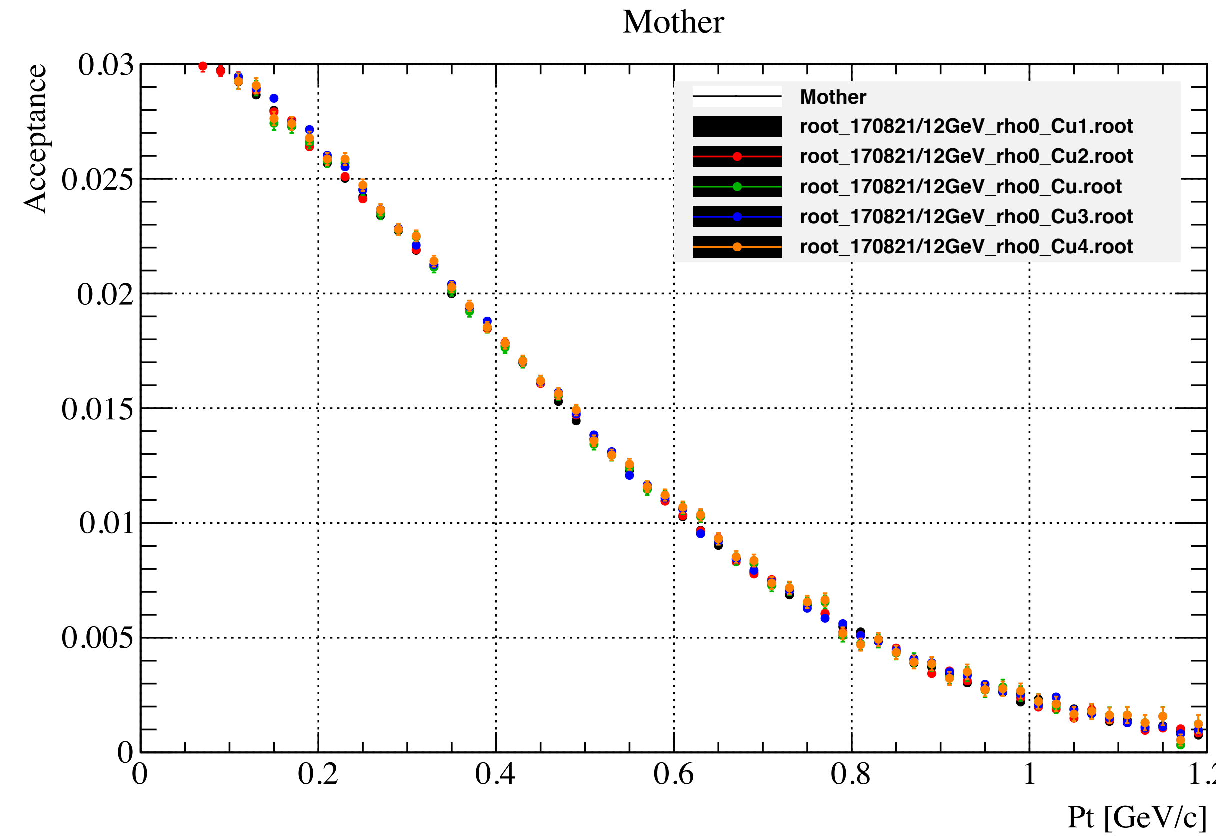

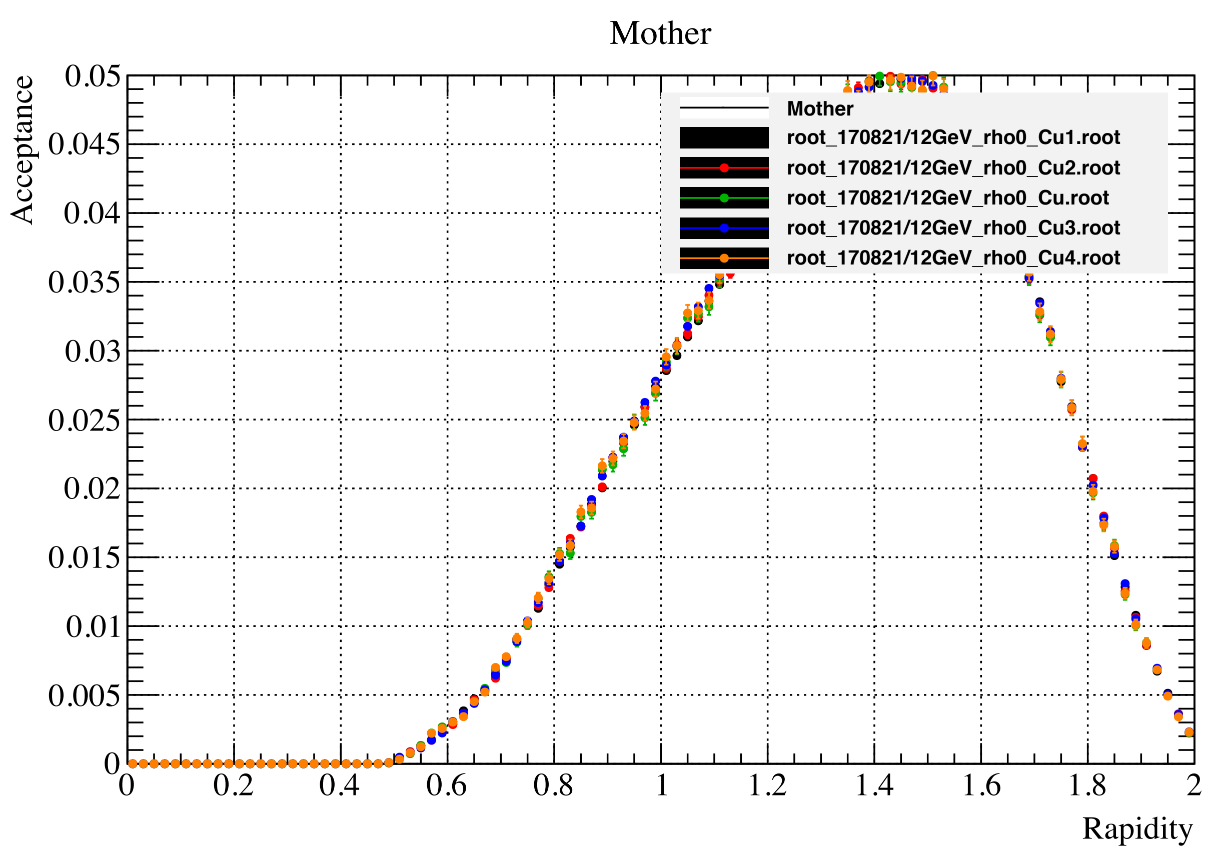

- Aligned for all the axis (bg, pt, and rapidity)

rho-omega interference

$$|F|^2 = \left| \frac{1}{m^2 - m_\rho^2 + im\Gamma_\rho^{tot}} + \frac{R}{m^2 - m_\omega^2 + im\Gamma_\omega^{tot}} \right|^2$$

$$R = \sqrt{\frac{\Gamma_\omega^{tot}}{\Gamma_\rho^{tot}}} \cdot \sqrt{\frac{\sigma_\omega \mathrm{Br}(\omega \to e^+e^-)}{\sigma_\rho \mathrm{Br}(\rho \to e^+e^-)}} \times e^{i\theta}$$

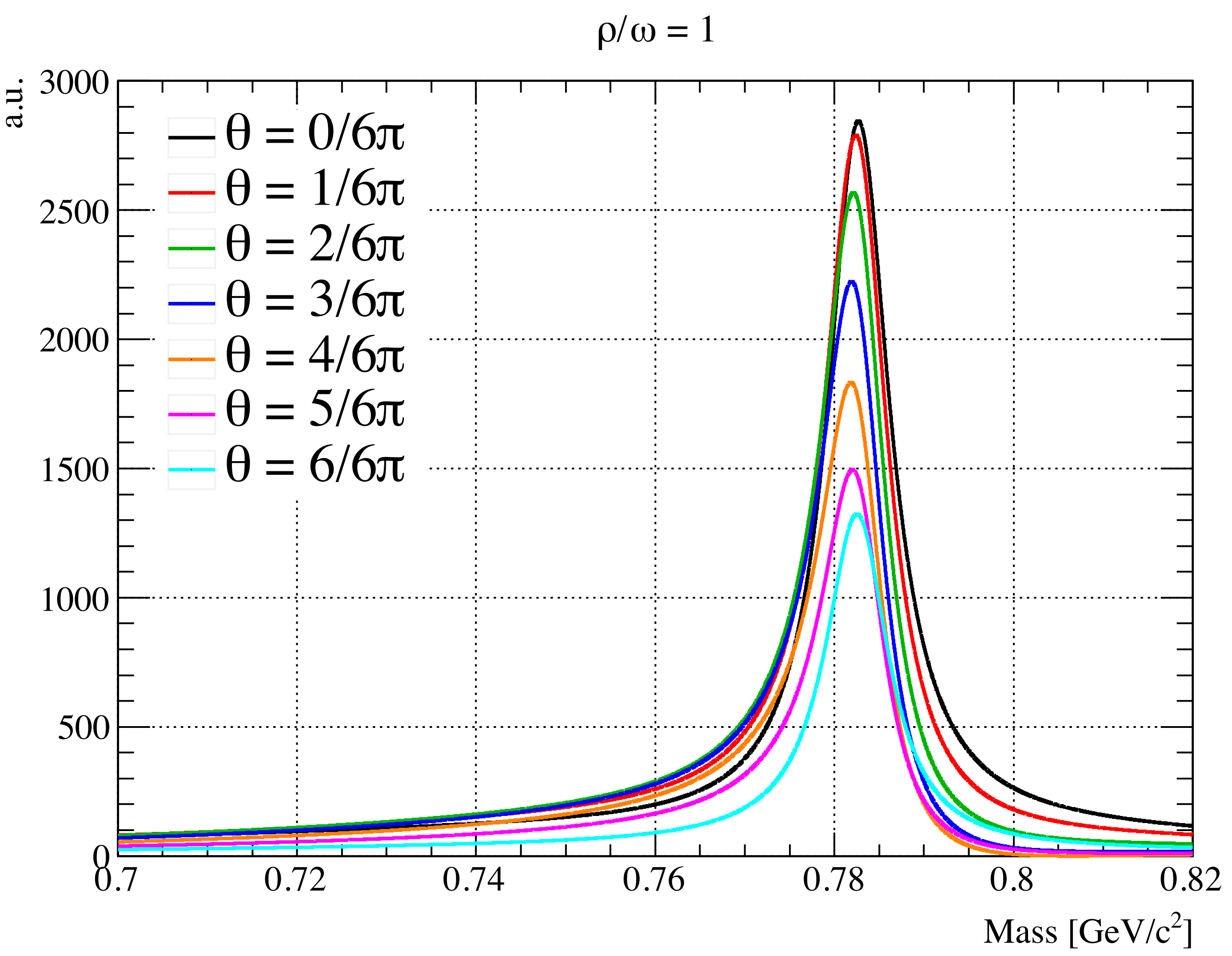

- F. M. Renard. rho-omega mixing. In G. Hoehler, editor, Springer Tracts in Modern Physics, volume 63, page 98. Springer-Verlag GmbH, 1972.
- $\theta = 2$ radian is favored by some theory. (Private communication w/ R. Veenhof)
- No need to consider $\theta > \pi$ region (Obviously high-mass tail will not fit the data)

ρ-ω interference
chi2 vs (theta, r/w)

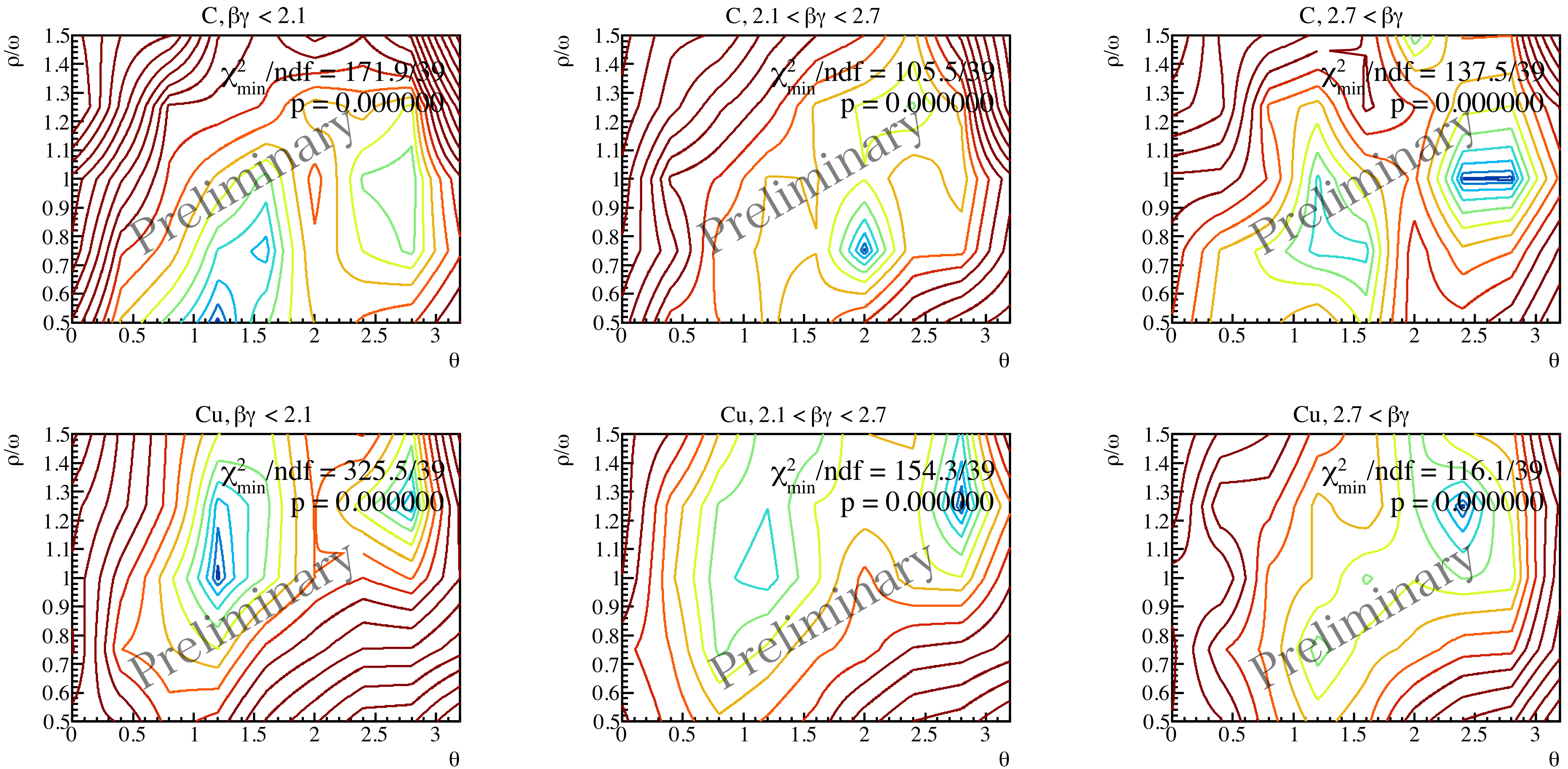

- The parameters were not common for C, Cu, and for each bg region.
- The best chi2 values were very large.

Excess ratio vs bg

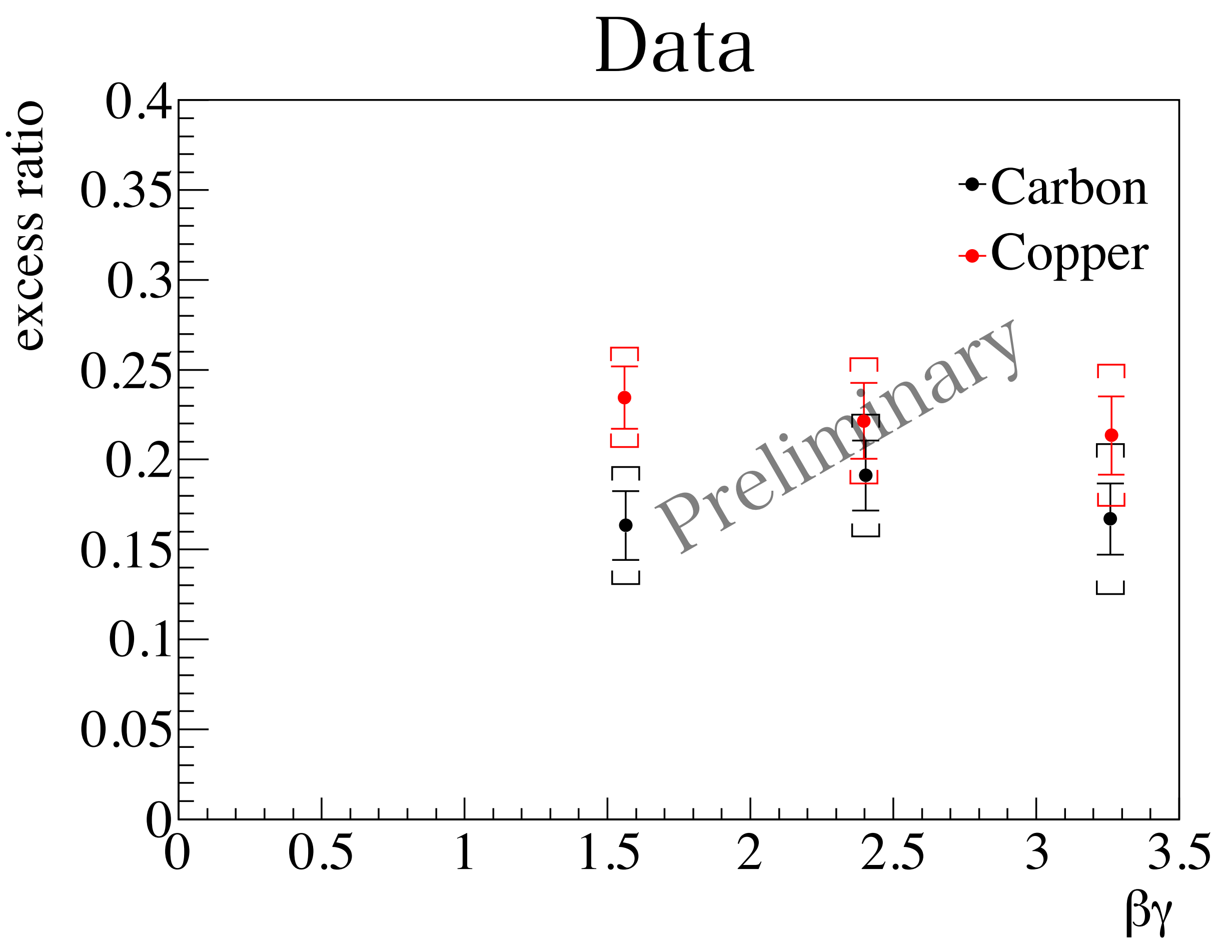

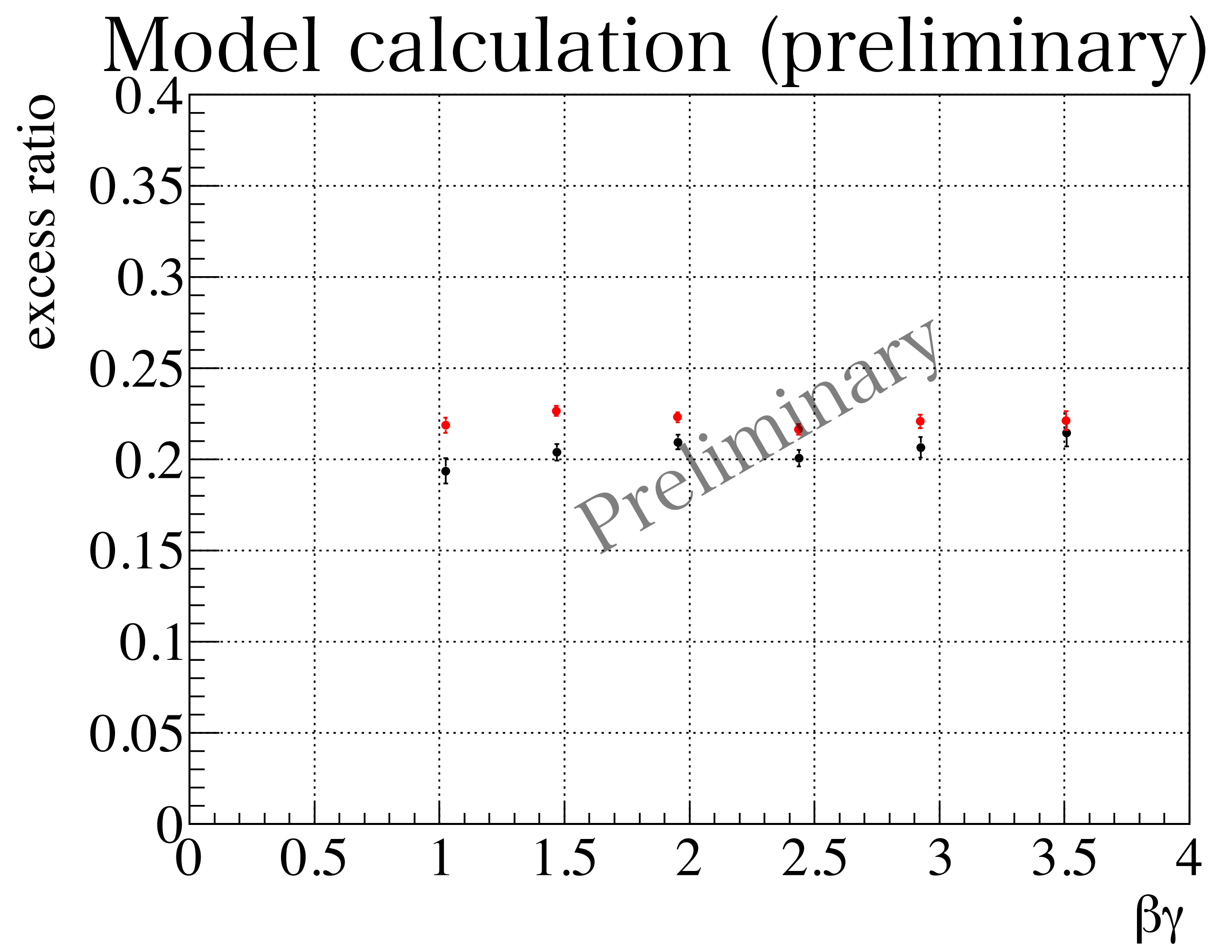

- In the model calculation, the model parameters were fixed as k1 = 0.12, k2 = 0.0, rho/omega ratio = 1.0
- nBW/m^3 was used for the mass function.